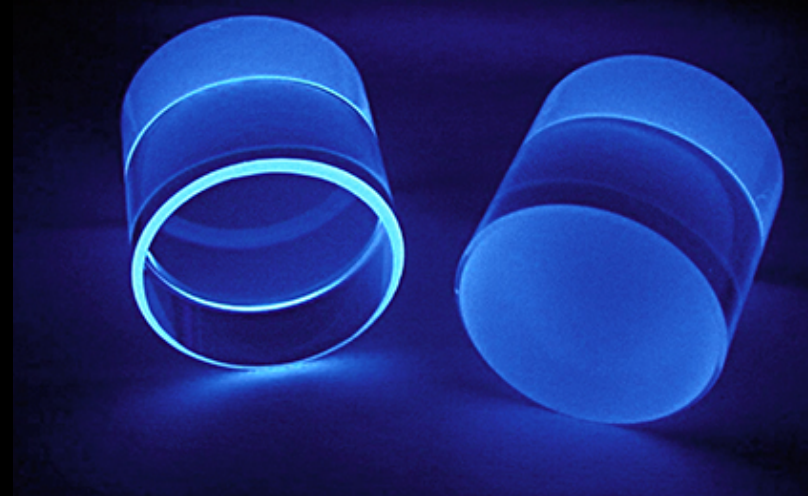
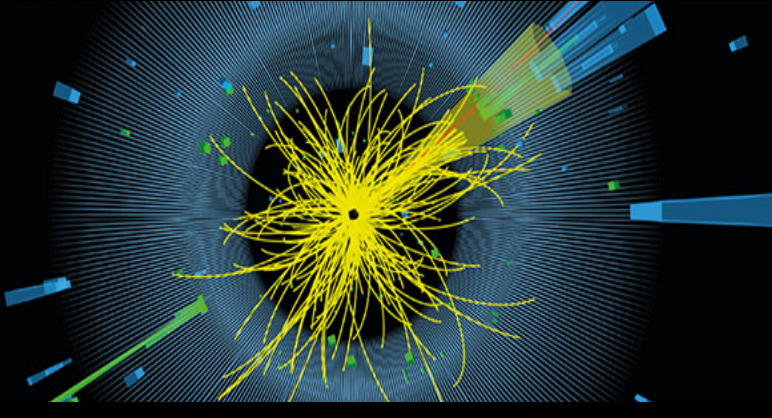
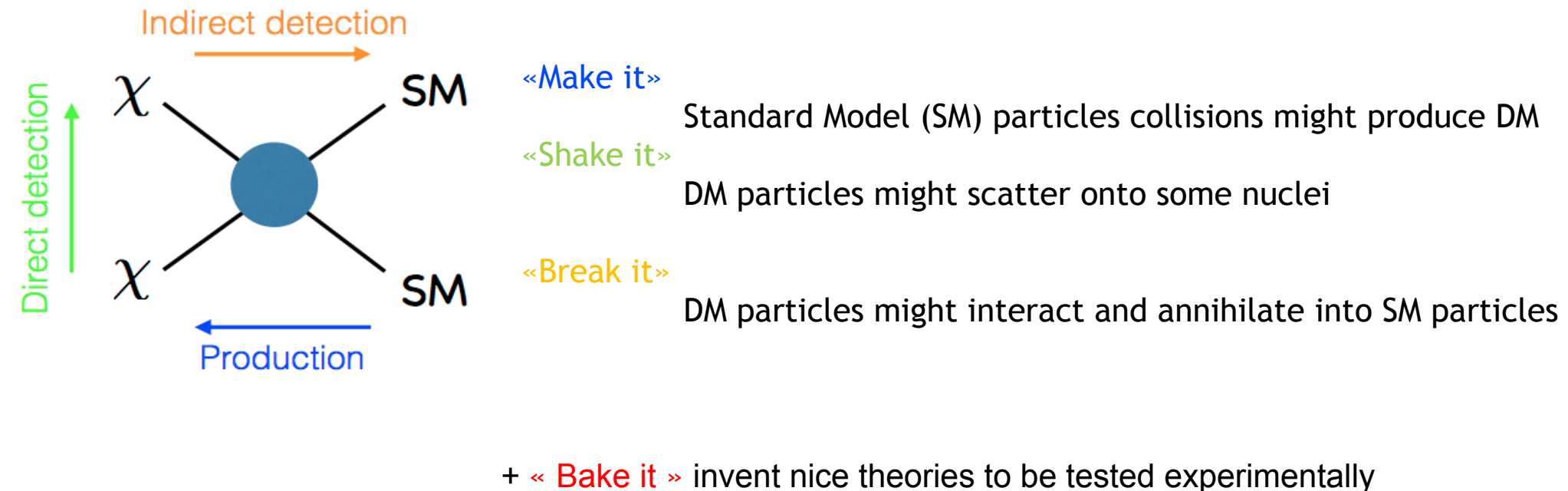


Searches for Dark Matter



Astro Particle Physics
WS 2020/2021 - 14th January 2021
Federico Ambrogi (dep. Meteorology, Univie)

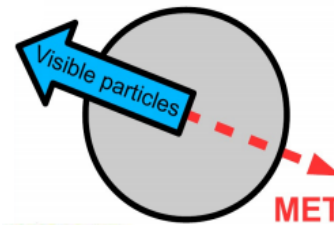
If we are finally convinced that Dark Matter exists... how do we search for it?



Example: SUSY at the LHC

- Assumption: all the SUSY particles will eventually decay to the lightest Neutralino, which is the DM candidate here considered, and it *escapes detection* since *it does not interact with the detector*
- This will produce “missing transverse energy” (MET) i.e. an energy imbalance in the event

$$E_T^{\text{miss}} = |\vec{p}_T^{\text{miss}}| = \left| \sum_i \vec{p}_T^i \right|$$



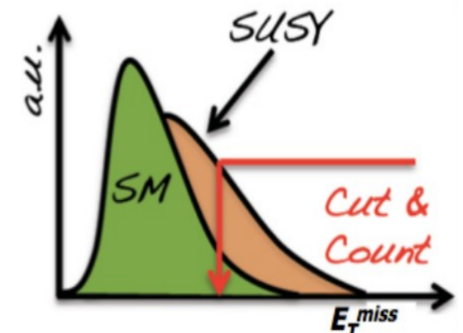
What we “see”

What we do not “see”

-> The presence of a DM candidate in the events (i.e. each interaction recorded at the detector), will produce an imbalance in the total energy/momentum of the visible particles

<https://atlas.cern/updates/blog/what-happens-when-energy-goes-missing>

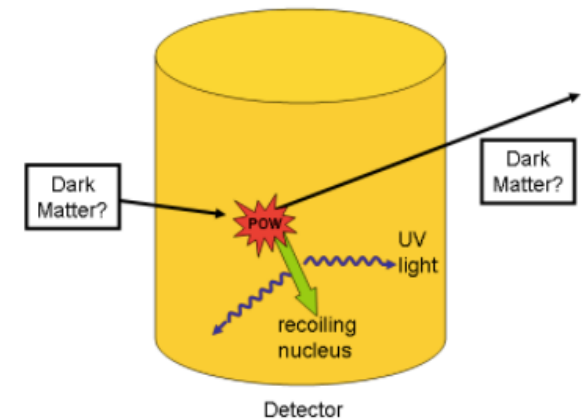
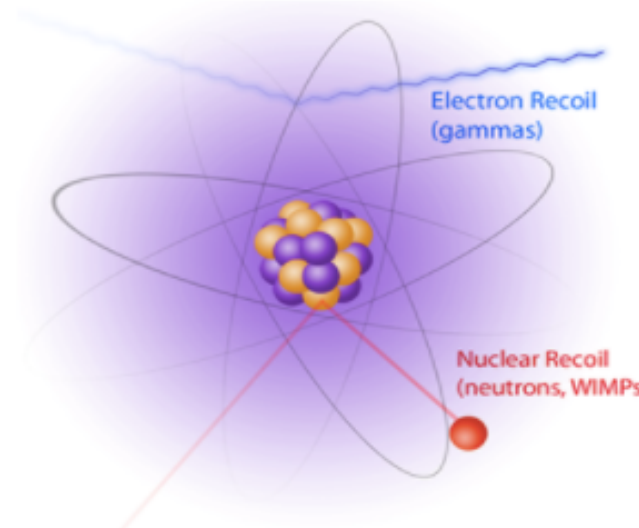
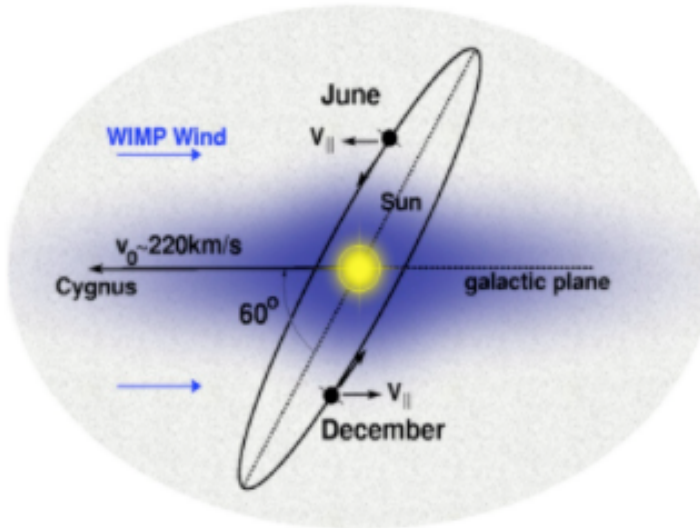
<https://physics.stackexchange.com/questions/61194/what-is-transverse-energy>



Direct Detection

« Shake it » : DM Direct Detection

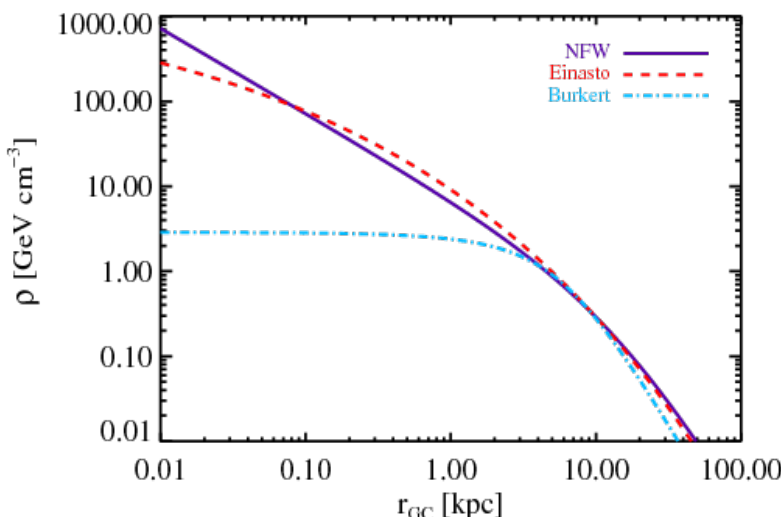
- Idea: the Earth travels through the DM Milky Way's halo, and DM particles might scatter off (heavy) nuclei



- Idea: the Earth travels through the DM Milky Way's halo, and DM particles might scatter off (heavy) nuclei
- In general, the expected event rate can be expressed as

$$\frac{dR}{dE}(E, t) = \frac{\rho_0}{m_\chi m_A} \int v \cdot f(\mathbf{v}, t) \cdot \frac{\sigma}{dE}(E, v) d^3v$$

Models for the Halo densities



$$\rho(r)_{DM} = \left(\rho_\odot \frac{R_\odot}{R} \right)^\gamma \left(\frac{1+(R_\odot/a)^\alpha}{1+(r/a)^\alpha} \right)^{(\beta-\alpha)/\gamma}$$

Profile	α	β	γ
Isothermal	2	2	0
NFW	1	3	1
Moore	1.5	3	1.5

where a is a fit parameters related to the halo scale, $R_\odot = 8.5$ kilo Parsec is the distance of the Sun from the galactic center, and $\rho_\odot \approx 0.3$ [GeV cm⁻³] is the local DM density .

The precise shape of the density profile for $r \rightarrow 0$ is unknown and different possibilities were derived from N-body simulations. Some solutions exhibit a flat core, others are more cuspy. Recent studies of dwarf galaxies indicate that the “cuspyness” of the density profile depends on the star formation rate which drives fluctuations in the gravitational potential: galaxies with longer lasting star formation have more shallow dark matter cores”

<https://arxiv.org/pdf/1903.03026.pdf>

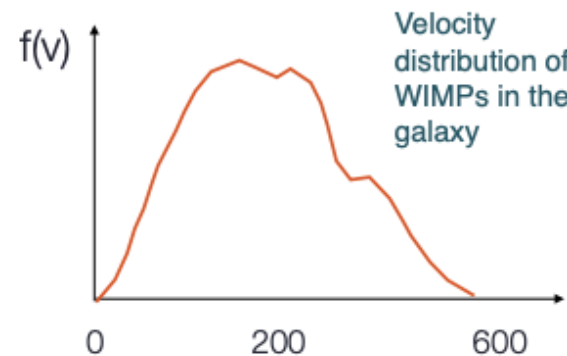
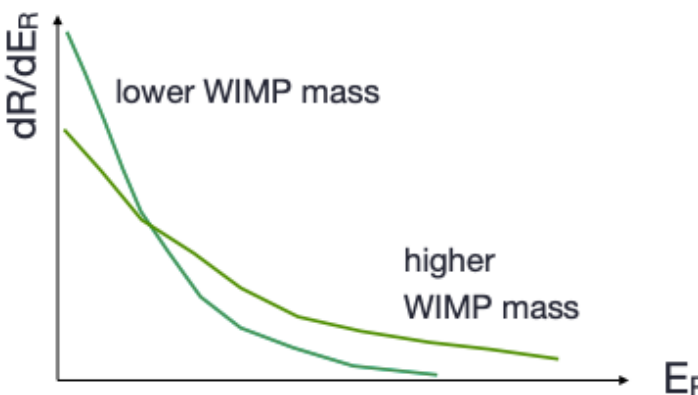
- Idea: the Earth travels through the DM Milky Way's halo, and DM particles might scatter off (heavy) nuclei
- In general, the expected event rate can be expressed as

$$\frac{dR}{dE}(E, t) = \frac{\rho_0}{m_\chi m_A} \int v \cdot f(\mathbf{v}, t) \cdot \frac{\sigma}{dE}(E, v) d^3v$$

m_χ = DM mass

m_A = mass of the atomic species

- local density $\rho_0 \equiv \rho(R_0) = 0.3 \text{ GeV cm}^{-3}$
- local circular speed $v_c = 220 \text{ km s}^{-1}$



https://indico.cern.ch/event/630418/contributions/2813742/attachments/1577606/2491733/aprile_ICFA_Lecture1.pdf

Key points for DM Direct detection:

- DM induced recoils energies are very small (eV ~ keV range)
- Many natural signals can mimic DM scattering e.g. background neutrinos (Sun, radioactive decays...)
- Accurate signal/background discrimination needed
- On the side: they can study DM & other physics at the same time (e.g. neutrino physics, extremely rare radioactive decays)
- Limitation: neutrino floor

Experimental strategies:

- Noble liquid targets
[DARWIN, LUX, Panda-X, XENON, XENON1T, XENONnT , ...]
- Cryogenic Crystal Targets
[CRESST(II,III) , EDELWEISS, SuperCDMS, ...]
- Others: e.g. bubble chambers, NaI crystals
[ANAIS, DAMA/LIBRA(sodium-iodine crystals), COSINE, PICO...]

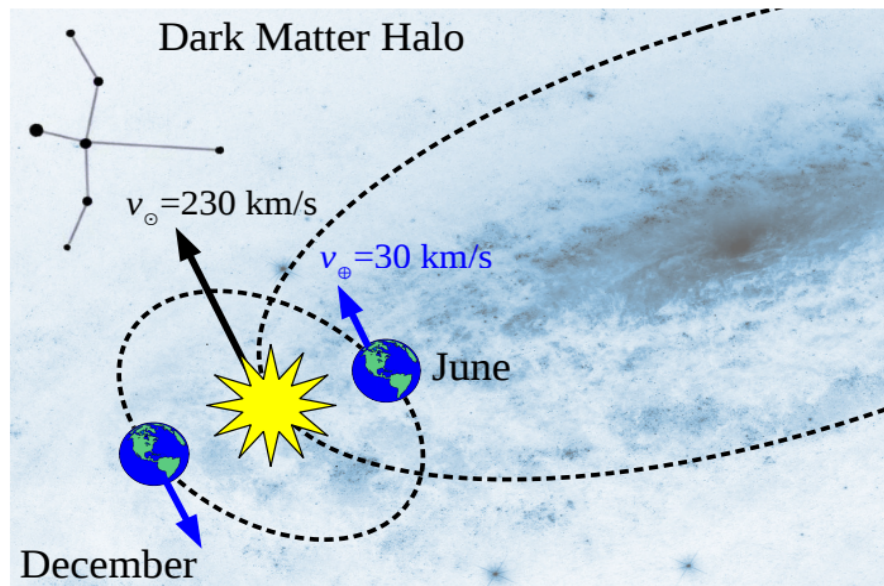


Figure 4. Illustration of the Sun-Earth system moving around the galactic center and through the dark matter halo in the direction of the constellation Cygnus. The varying vector addition of the velocities over the course of a year is expected to induce a modulating dark matter signature.

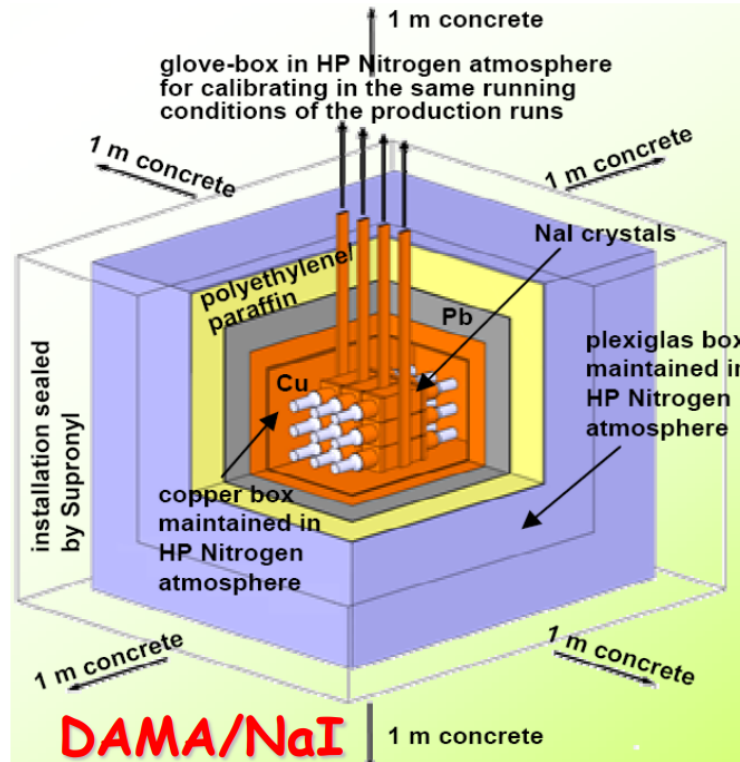
Evidence suggests that both the Sun and the Earth are enveloped by the Dark Matter halo of the Milky Way.

As the Earth's velocity relative to the Sun varies over its one-year orbit, so does its velocity relative to the Dark Matter.

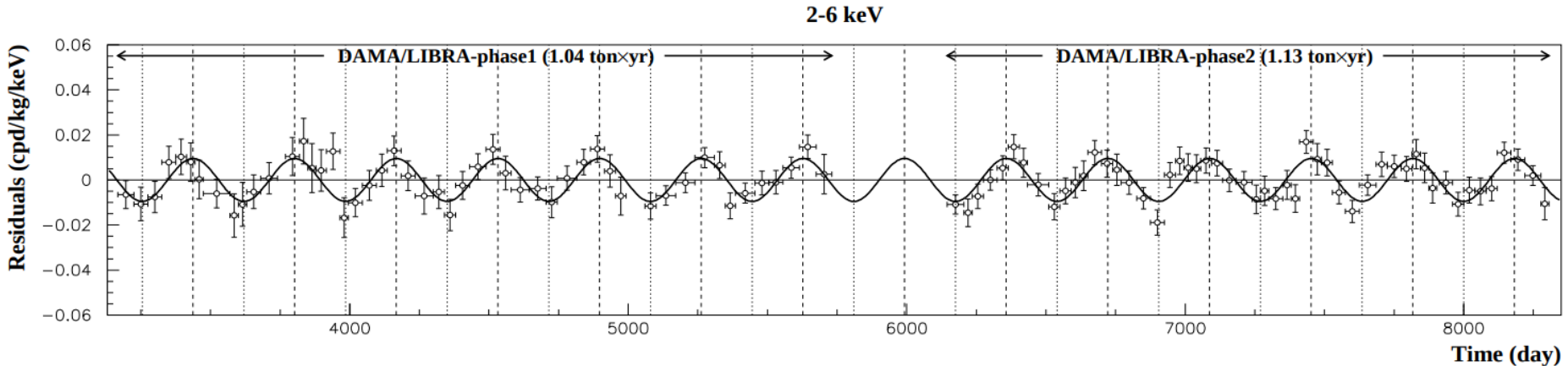
This should result in the so-called “WIMP wind” that blows harder in June, and softer in December.

[Halo is assumed to be static]

<https://science.purdue.edu/xenon1t/?tag=annual-modulation>



- 25 highly radiopure scintillating thallium-doped sodium iodide (NaI(Tl)) crystals
- detectors are placed inside a sealed copper box flushed with highly pure nitrogen;
- multi-ton shield to reduce the natural environmental background .
- + 1 m of Gran Sasso rock material



The data of the new DAMA/LIBRA-phase2 confirm a peculiar annual modulation in the (1-6) keV energy region:

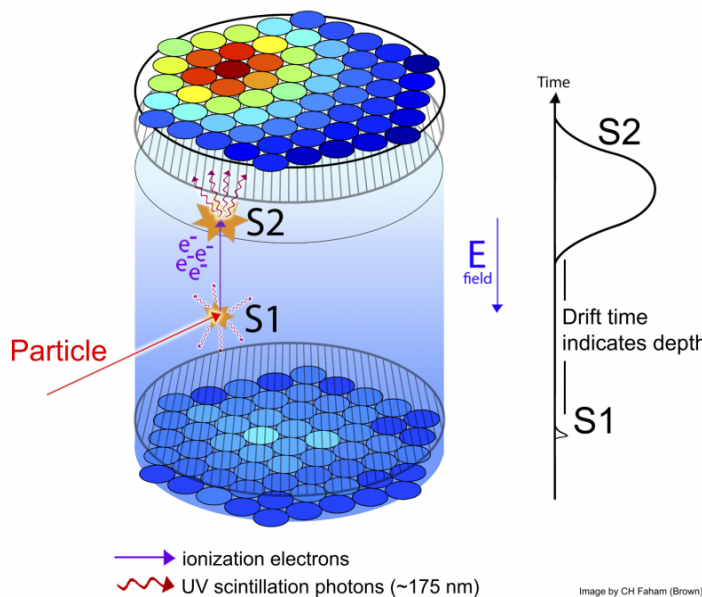
- 1) clear cosine-like modulation
- 2) the measured period is equal to (0.999 ± 0.001) yr well compatible with the 1 yr period as expected for the DM signal
- 3) the measured phase (145 ± 5) days is compatible with the roughly ≈ 152.5 days expected for the DM signal
- 4) the modulation is present only in the low energy (1-6) keV interval and not in other higher energy regions
- 5) the modulation is present only in the single-hit events, while it is absent in the multiple-hit ones as expected for the DM signal

...

No systematic or side processes able to mimic the signature (...) has been found

Thus, on the basis of the exploited signature, the model independent DAMA results give evidence at **12.9σ C.L.** (over 20 *independent annual cycles* and in various experimental configurations) for the presence of DM particles in the galactic halo

<https://www.lngs.infn.it/en/dama-eng>



LUX is a dual-phase liquid/gas xenon Time Projection Chamber (TPC) [South Dakota]. When a WIMP (or other particle e.g. neutron) interacts with one of the xenon atoms in the liquid portion of the detector, it causes the xenon nucleus to recoil (**S1** signal).

The recoil leads to a burst of scintillation light (175 nm ultraviolet) and to the ionization of the surrounding xenon atoms \rightarrow ionization electrons

Electrons drift to the top of the detector (electric field) where they encounter the gas-liquid interface, and produce a second burst of light through electroluminescence (**S2**).

The resultant photons from each burst of light are detected by 122 Photomultiplier Tubes (PMTs), split between the top and bottom of the detector.

The two signals, S1 and S2, are separated by the drift time of the electrons, from which we can infer the location of the event by combining with the geometrical patterns produced by the number of photoelectrons detected by each PMT.

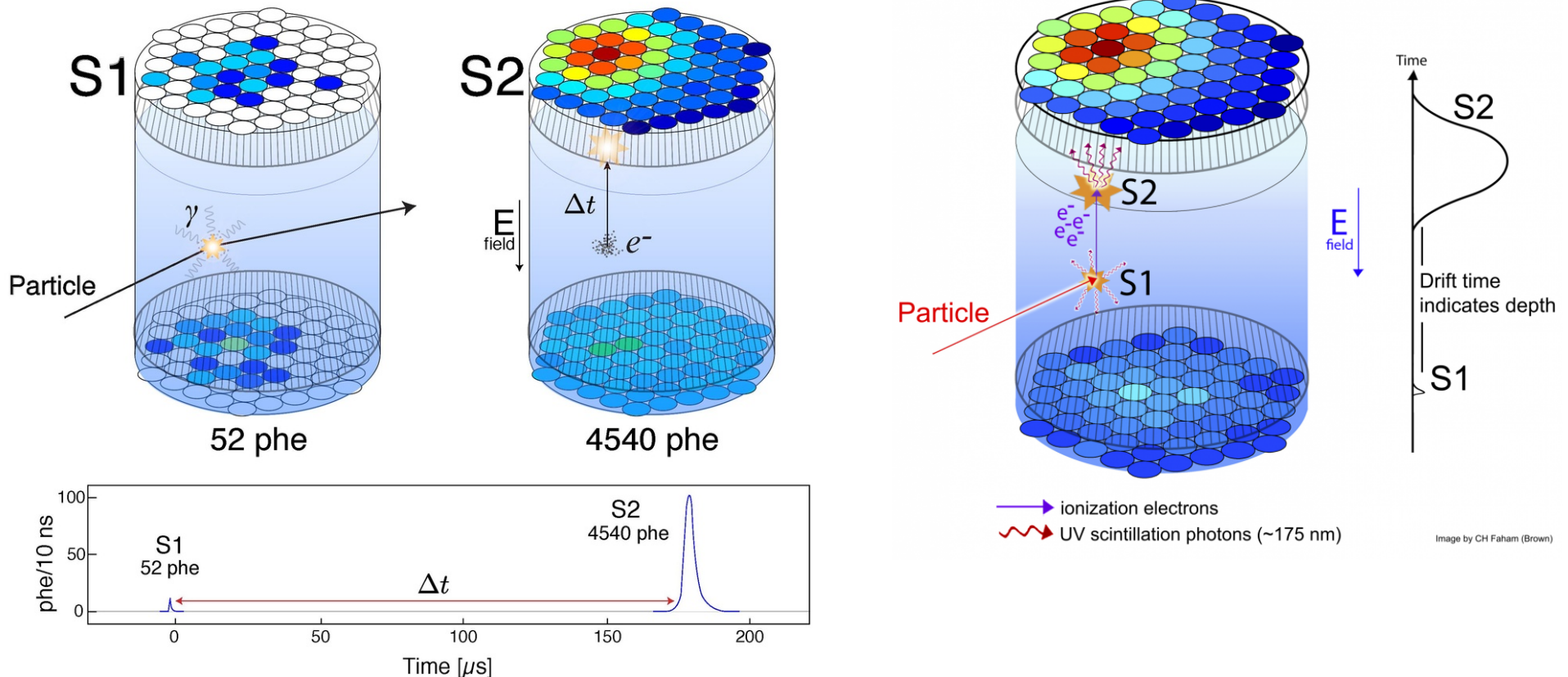
This position information is vital for discrimination between signal and background since the xenon self-shielding causes most of the background events to be concentrated near the walls of the detector.

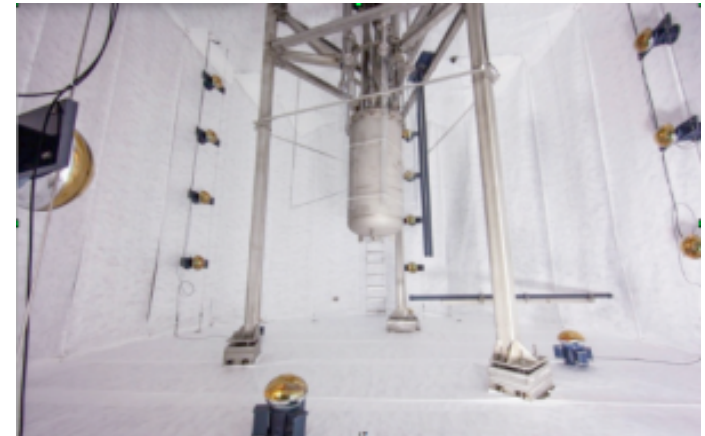
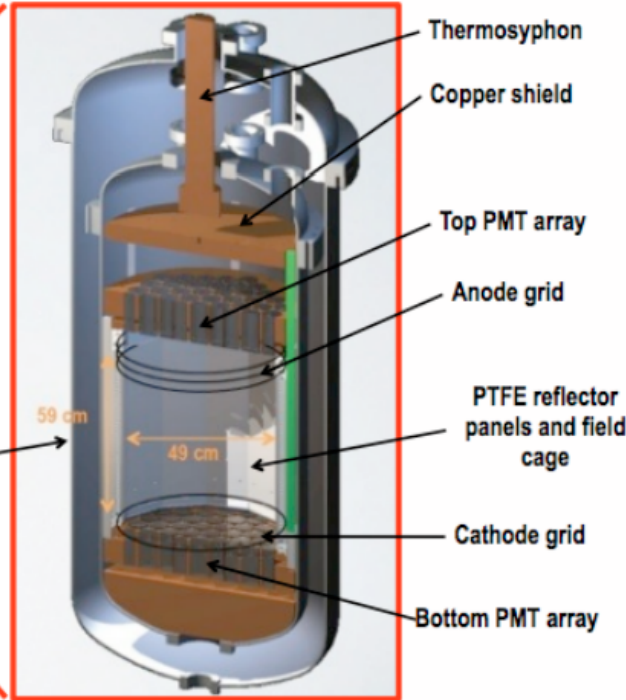
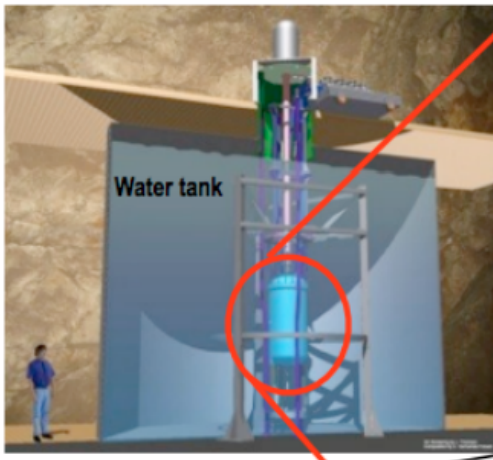
Uniform backgrounds such as the decays of radioactive elements contaminating the xenon itself, will produce electron-recoils rather than nuclear recoils in the detector.

These events can be distinguished from that of nuclear recoils based on the ratios of their S1 and S2 signals.

<https://www.hep.ucl.ac.uk/darkMatter/>

[For Xenon1T: the electrons are drifted by an electric field to the liquid-gas interface with a speed of about 2 mm/ μ s.]





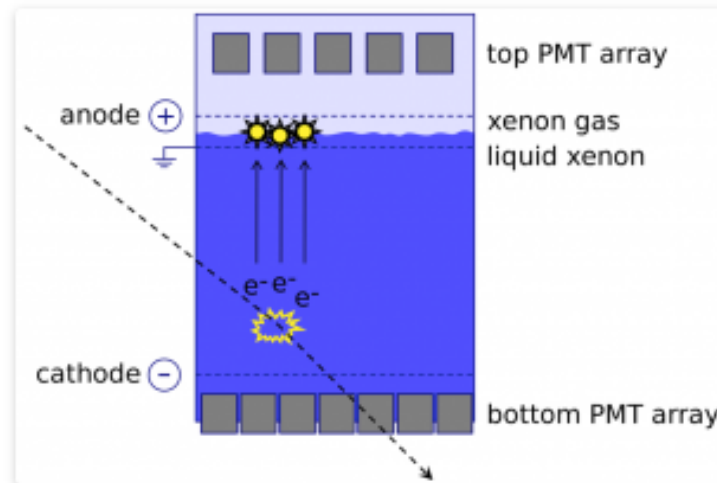


- 3.2 tons of ultra radio-pure liquid Xenon
- Fiducial volume of about 2 tons
- The detector is housed in a 10 m water tank that serves as a muon veto
- The TPC is 1 m in diameter and 1 m in height

“In April 2019, based on measurements performed with the XENON1T detector, the XENON Collaboration reported in [Nature](#) the first direct observation of two-neutrino [double electron capture](#) in xenon-124 nuclei...

The measured half-life of this process, which is several orders of magnitude larger than the age of the Universe, demonstrates the capabilities of xenon-based detectors to search for rare events and showcases the broad physics reach of even larger next-generation experiments.

This measurement represents a first step in the search for the [neutrinoless double electron capture](#) process, the detection of which would provide valuable insight into the nature of the [neutrino](#) and allow to determine its absolute mass”



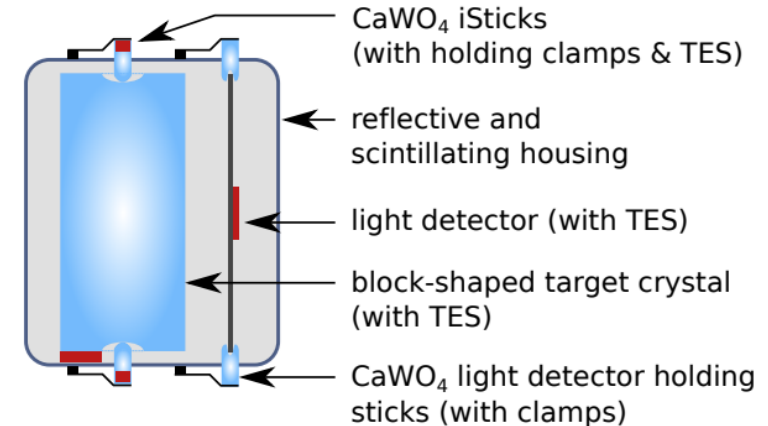
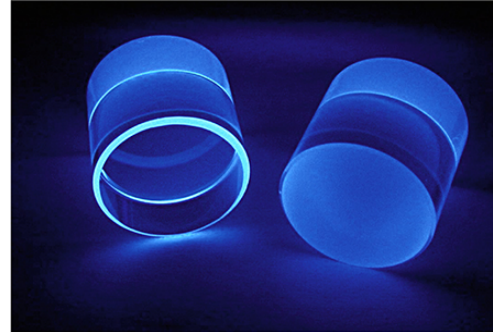
Schema of the XENON experiment: any particle interaction in the liquid xenon (blue) yields two signals: a prompt flash of light, and a delayed charge signal. Together, these two signals give away the energy and position of the interaction as well as the type of the interacting particle. (Schema: The XENON collaboration/Rafael Lang)

An interaction in the target generates scintillation light which is recorded as a prompt signal (called S1) by two arrays of photomultiplier tubes (PMTs) at the top and bottom of the chamber. In addition, each interaction liberates electrons, which are drifted by an electric field to the liquid-gas interface with a speed of about $2 \text{ mm}/\mu\text{s}$. There, a strong electric field extracts the electrons and generates proportional scintillation which is recorded by the same photomultiplier arrays as a delayed signal (called S2). The time difference between these two signals gives the depth of the interaction in the time-projection chamber with a resolution of a few mm. The hit pattern of the S2 signal on the top array allows to reconstruct the horizontal position of the interaction vertex also with a resolution of a few mm. Taken together, our experiment is able to precisely localize events in all three coordinates. This enables the fiducialization of the target, yielding a dramatic reduction of external radioactive backgrounds due to the self-shielding capability of liquid xenon.

In addition, the ratio S2/S1 allows to discriminate electronic recoils, which are the dominant background, from nuclear recoils, which are expected from Dark Matter interactions. And of course, the more energy a particle deposits in the detector, the brighter both S1 and S2 signals are, hence allowing us to reconstruct the particle's deposited energy as well.

<http://www.xenon1t.org/>

CRESST (Cryogenic Rare Event Search with Superconducting Thermometers)



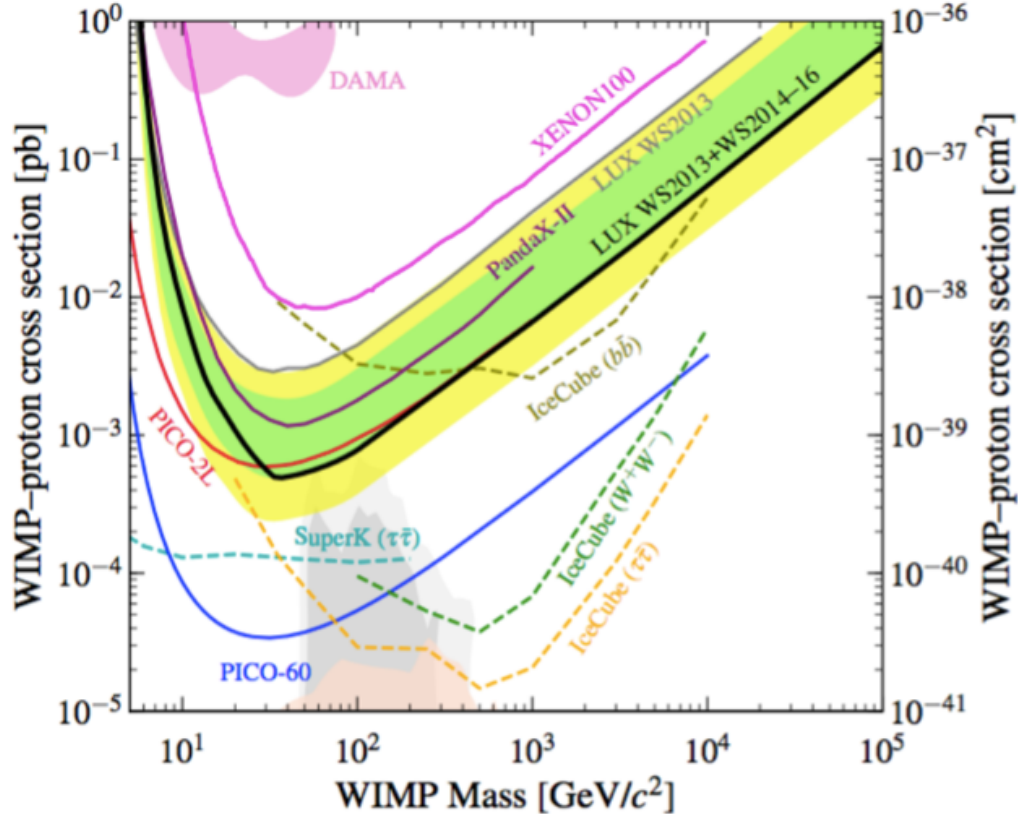
- The CRESST-III experiment operates scintillating CaWO₄ (calcium-tungstate) crystals as cryogenic calorimeters, simultaneously measuring a phonon/heat and a scintillation light signal.
- A distinctive feature of the phonon signal is a precise determination of the energy deposited in the crystal, independent from the type of particle interaction.
- This property, in combination with a low energy threshold, makes cryogenic calorimeters particularly suited **for low-mass dark matter detection**.
- Contrary to the phonon signal, the scintillation light strongly depends on the type of particle interaction, yielding event-by-event discrimination between the dominant background (β/γ -interactions) and the sought-for nuclear recoils.

- CRESST is located in the Laboratori Nazionali del Gran Sasso (LNGS) underground laboratory in central Italy which provides an overburden against cosmic radiation with a water equivalent of 3600 m
- Remaining muons are tagged by an active muon veto with 98.7% geometrical coverage
- In addition, the experimental volume is protected by concentric layers of shielding material comprising - from outside to inside - polyethylene, lead and copper.
- The polyethylene shields from environmental neutrons, while lead and copper suppress γ -rays.
- A second layer of polyethylene inside the copper shielding guards against neutrons produced in the lead or the copper shields. A commercial $^3\text{He}/^4\text{He}$ -dilution refrigerator provides the base temperature of about 5 mK. Cryogenic liquids (LN₂ and LHe) are refilled three times a week causing a down-time of about 3 h per refill.

<https://www.oeaw.ac.at/en/hephy/research/dark-matter-experiment/cresst>

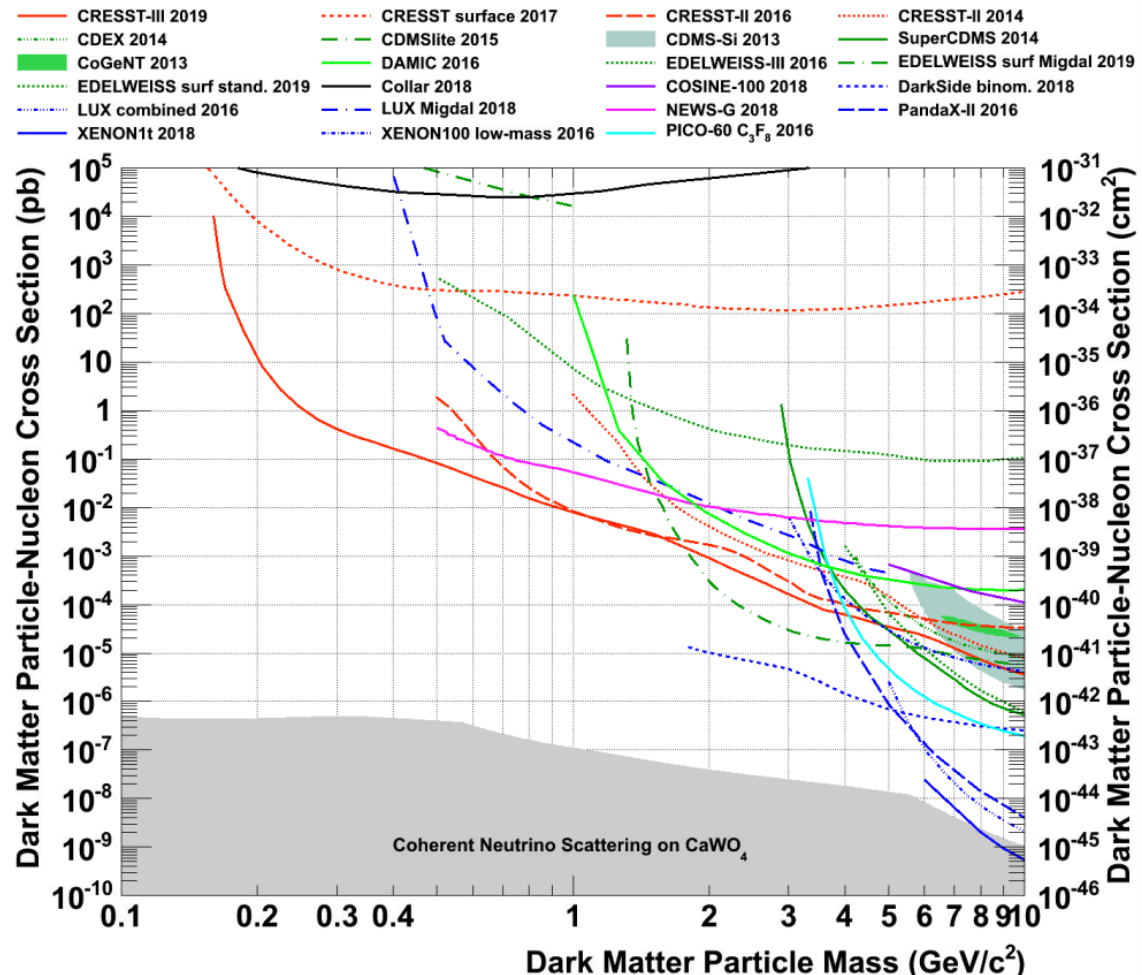


Results



$$\frac{dR}{dE}(E, t) = \frac{\rho_0}{m_\chi m_A} \int v \cdot f(\mathbf{v}, t) \cdot \frac{\sigma}{dE}(E, v) d^3v$$

Results



- When a neutrino scatters off a nucleus, the interaction depends on the neutrino-nucleon interaction
- for small momentum transfer it does not resolve the internal structure of the nucleus (i.e. does not see nucleons)
- the neutrino scatters off the nucleus as a whole
- give rise to a coherent enhancement of the scattering cross-section
- neutral-current process: experimental signature is nuclear recoils with energies of only few eV to keV.

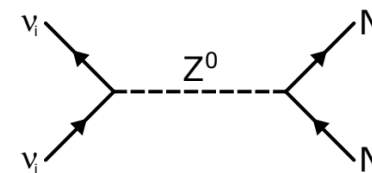
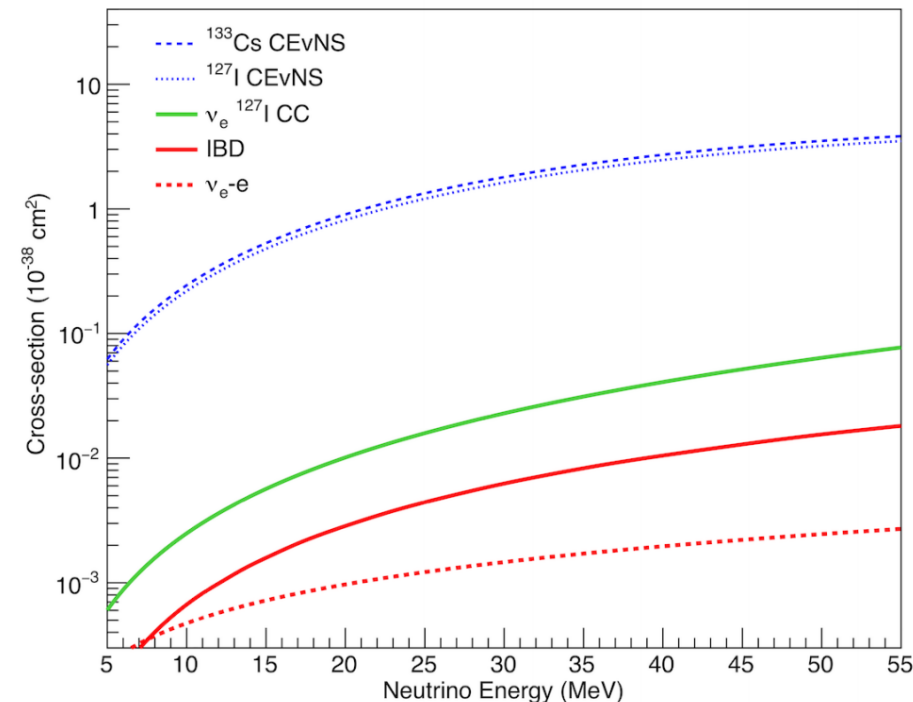


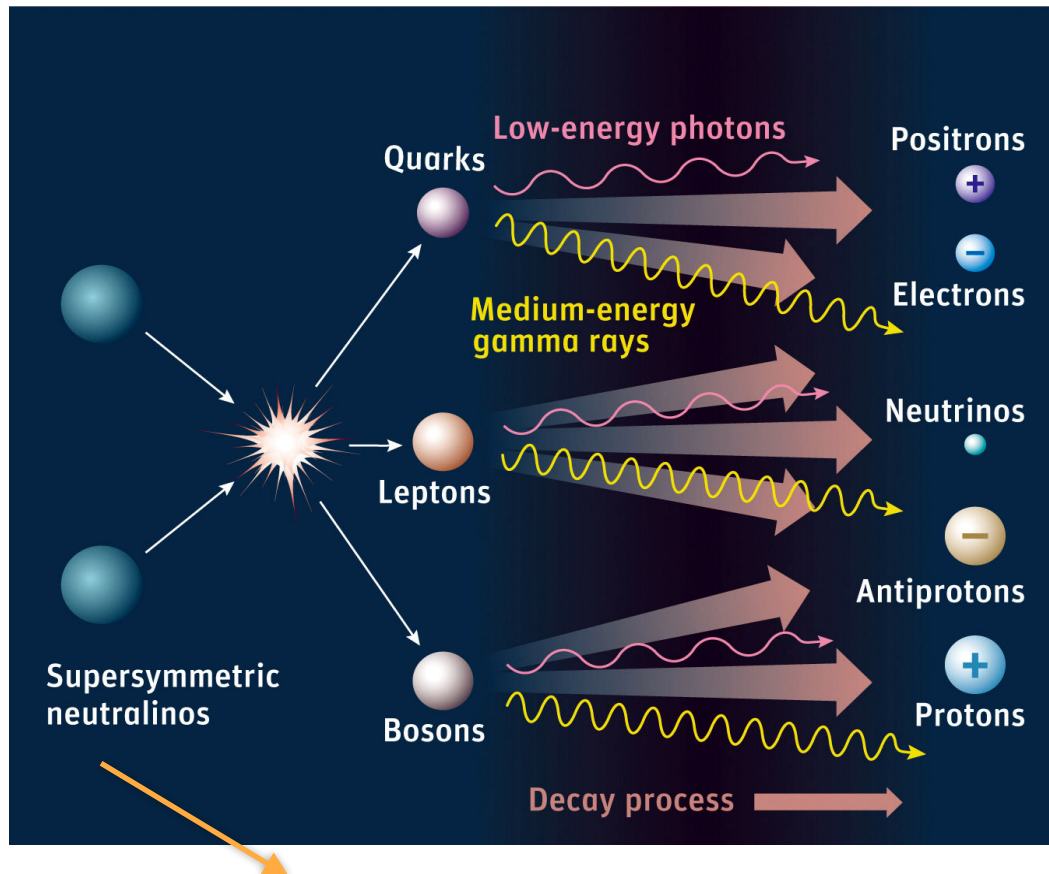
Figure 2.1: Feynman diagram for $\text{CE}\nu\text{NS}$. Here ν_i describes both neutrinos and anti-neutrinos of any flavor and N denotes any nucleus.

... Essentially the same happens
in the case of WIMPS !

Figure 1.1: Total cross-section for $\text{CE}\nu\text{NS}$ (blue) and other neutrino couplings. Shown are the cross-sections from charged-current (CC) interaction with iodine (green), inverse beta decay (red) and neutrino-electron scattering (dotted red). It is readily visible that $\text{CE}\nu\text{NS}$ provides the largest cross-section, dominating over any charged-current interaction for incoming neutrino energies of less than 55 MeV. Plot adapted from [5].

<https://arxiv.org/pdf/1904.01155.pdf>

Direct Detection



- Idea: DM particles can interact and produce visible SM particle
- Ideal environments: regions with expected **large DM density**
 - Galactic centre
 - **Dwarf Spheroidal Galaxies**

Dwarf Spheroidal Galaxies (Milky Way Satellites)

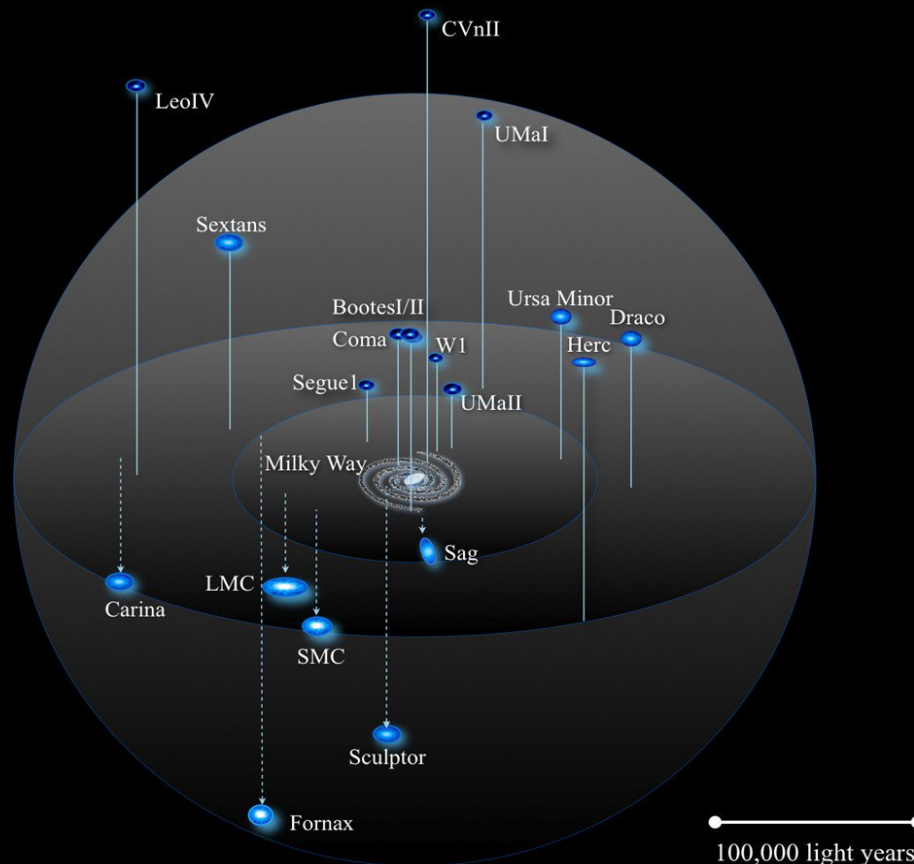
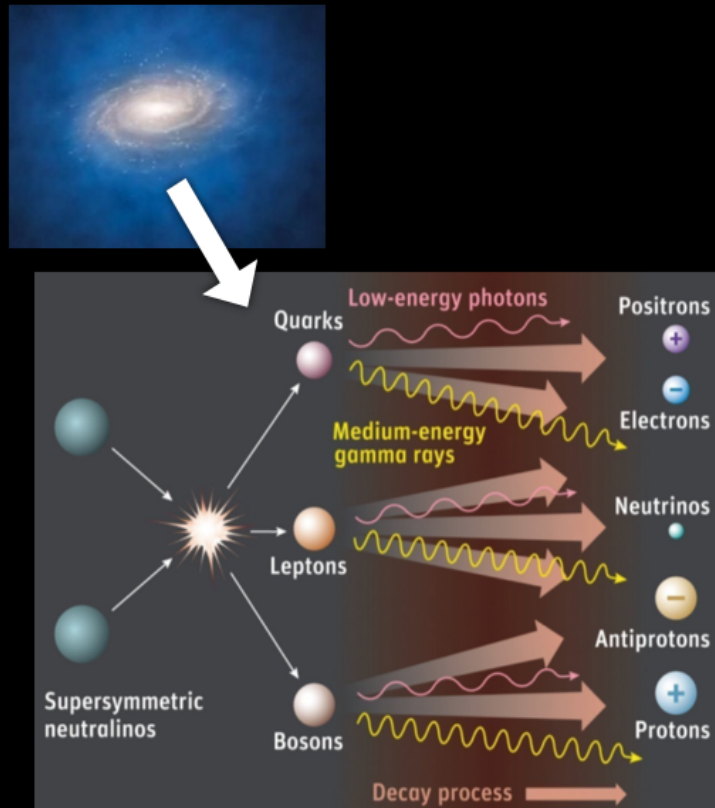


TABLE I. Properties of Milky Way dSphs.

Name	ℓ^a (deg)	b^a (deg)	Distance (kpc)	$\log_{10}(J_{\text{obs}})^b$ ($\log_{10} [\text{GeV}^2 \text{ cm}^{-5}]$)	Ref.
Bootes I	358.1	69.6	66	18.8 ± 0.22	[41]
Canes Venatici II	113.6	82.7	160	17.9 ± 0.25	[42]
Carina	260.1	-22.2	105	18.1 ± 0.23	[43]
Coma Berenices	241.9	83.6	44	19.0 ± 0.25	[42]
Draco	86.4	34.7	76	18.8 ± 0.16	[44]
Fornax	237.1	-65.7	147	18.2 ± 0.21	[43]
Hercules	28.7	36.9	132	18.1 ± 0.25	[42]
Leo II	220.2	67.2	233	17.6 ± 0.18	[45]
Leo IV	265.4	56.5	154	17.9 ± 0.28	[42]
Sculptor	287.5	-83.2	86	18.6 ± 0.18	[43]
Segue 1	220.5	50.4	23	19.5 ± 0.29	[46]
Sextans	243.5	42.3	86	18.4 ± 0.27	[43]
Ursa Major II	152.5	37.4	32	19.3 ± 0.28	[42]
Ursa Minor	105.0	44.8	76	18.8 ± 0.19	[44]
Willman 1	158.6	56.8	38	19.1 ± 0.31	[47]
Bootes II ^c	353.7	68.9	42	—	—
Bootes III	35.4	75.4	47	—	—
Canes Venatici I	74.3	79.8	218	17.7 ± 0.26	[42]
Canis Major	240.0	-8.0	7	—	—
Leo I	226.0	49.1	254	17.7 ± 0.18	[48]
Leo V	261.9	58.5	178	—	—
Pisces II	79.2	-47.1	182	—	—
Sagittarius	5.6	-14.2	26	—	—
Segue 2	149.4	-38.1	35	—	—
Ursa Major I	159.4	54.4	97	18.3 ± 0.24	[42]

^a Galactic longitude and latitude.

^b J-factors are calculated assuming an NFW density profile and integrated over a circular region with a solid angle of $\Delta\Omega \sim 2.4 \times 10^{-4} \text{ sr}$ (angular radius of 0.5°).



- DM annihilates inside galactic halos
- Typically 2-to-2 processes are considered i.e. $\chi \chi \rightarrow \text{SM SM}$ (called Simplified Models)

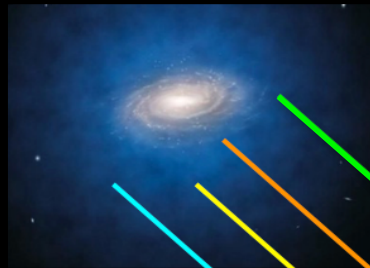
- From SM to Cosmic Rays (CR):

$$\gamma, \nu_e, \nu_\mu, \nu_\tau, e^+, \bar{p}$$

What is typically detected and analyzed

- CRs are detected at Earth (orbit)
e.g. Ice-cube, AMS, **Fermi-LAT**, ...
- Key observable: CRs **Differential energy spectrum**

$$\frac{d\Phi}{dE_\gamma}(E_\gamma, \psi)$$



DM annihilation in the halos
(external galaxies or in the Milky way)

ν_e γ
 ν_μ ν_τ

$$\frac{d\Phi}{dE_\gamma}(E_\gamma, \psi) = \frac{\langle\sigma v\rangle}{2m_\chi^2} \sum_i B_i \frac{dN_\gamma^i}{dE_\gamma} \frac{1}{4\pi} \int_\psi \frac{d\Omega}{\Delta\psi} \int_{\text{los}} \rho^2(\psi, l) dl$$

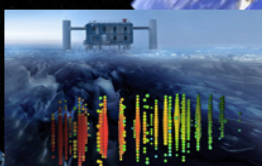
Velocity averaged annihilation cross section

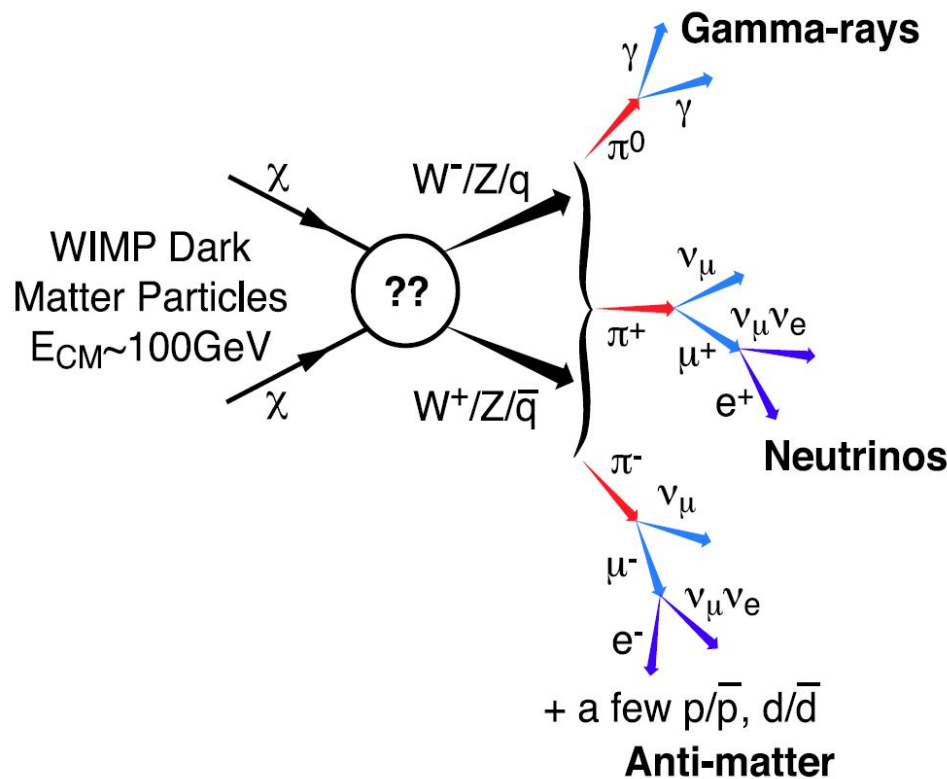
Energy spectra (summing over all the 'i' simplified channels)

J-factor from astrophysical observation

Fermi-LAT, ICECUBE,
AMS...

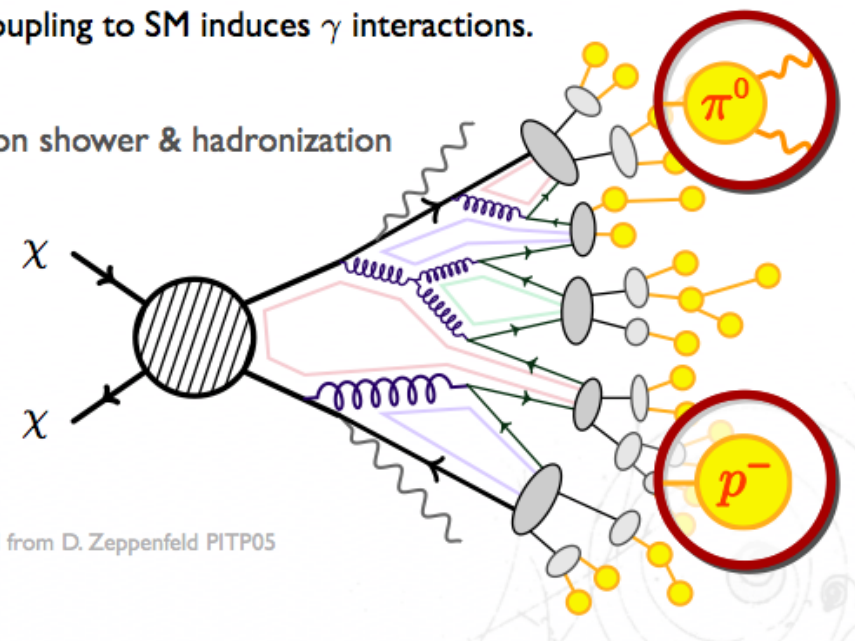
\bar{p}
 e^+





DM coupling to SM induces γ interactions.

Parton shower & hadronization



Adapted from D. Zeppenfeld PITP05

$\gamma, \nu_e, \nu_\mu, \nu_\tau, e^+, \bar{p}$

Fermi-LAT Large Array Telescope: focus on gamma rays (photons)



Fermi (formerly GLAST): two Instruments

The Large Area Telescope (LAT)

20 MeV - 300 GeV

>2.5 sr FoV



The Burst Monitor (GBM)

8 keV – 40 MeV

9.5 sr FoV



the LAT

modular - 4x4 array

7 ton – 650 watts

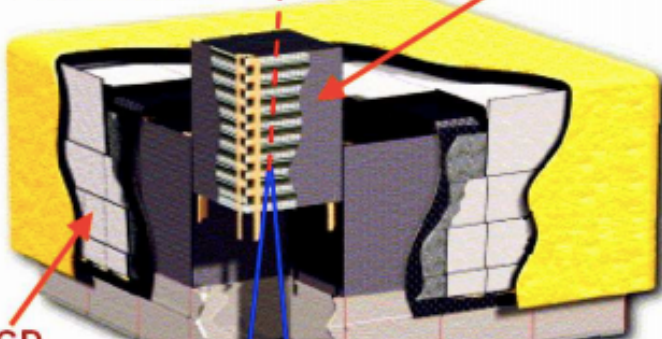
γ

ACD

Segmented Anticoincidence Detector (ACD) 89 plastic scintillator tiles. Rejects background of charged cosmic rays; segmentation mitigates self-veto effects at high energy.

Tracker (4x4 array of towers)

Precision Si-strip Tracker (TKR) 18 XY tracking planes with tungsten foil converters. Single-sided silicon strip detectors (228 μm pitch, 900k strips) Measures the photon direction; gamma ID.

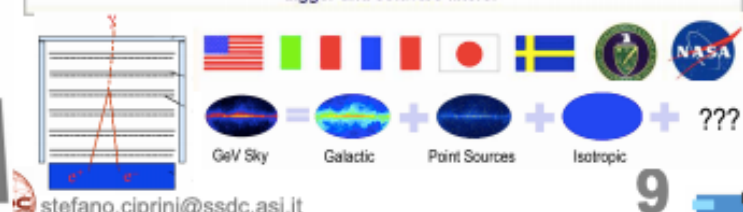


Calorimeter

Hodoscopic CsI Calorimeter (CAL) Array of 1536 CsI(Tl) crystals in 8 layers. Measures the photon energy; image the shower.

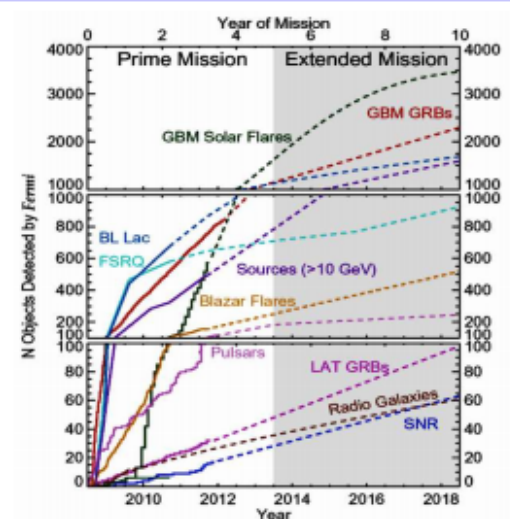
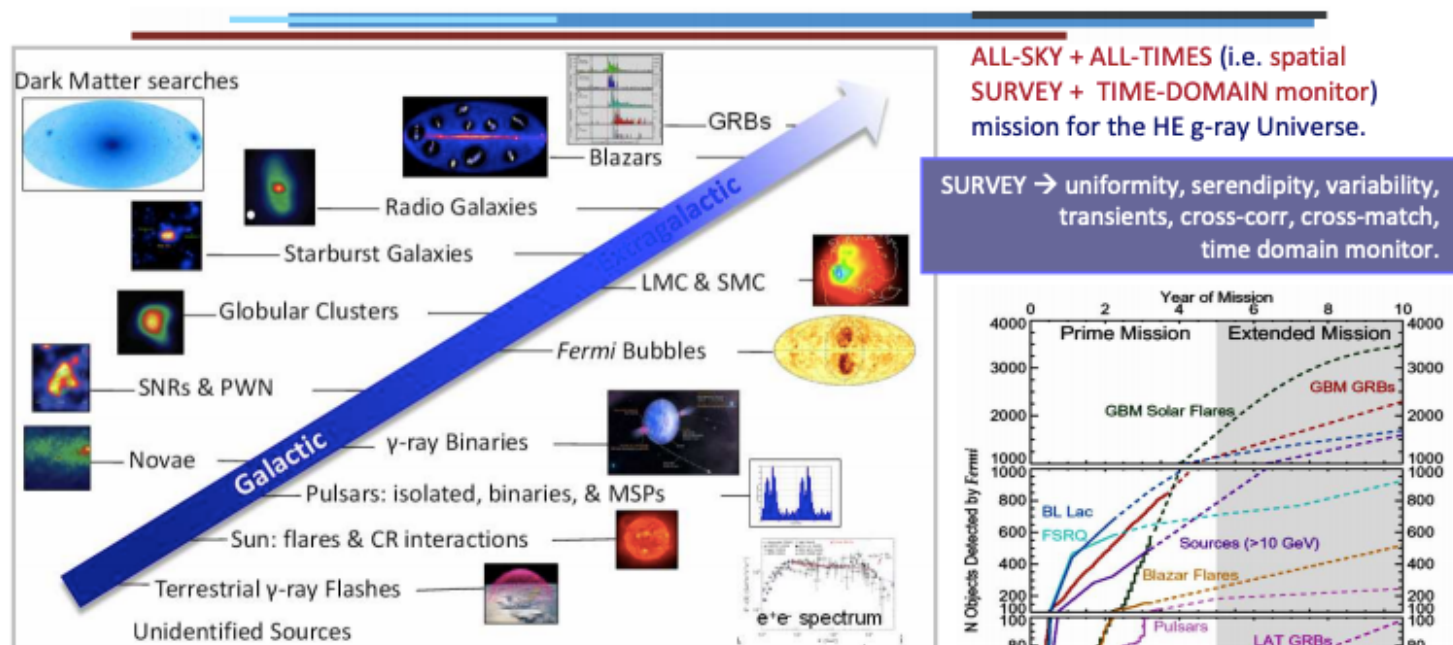
Electronics System

Includes flexible, robust hardware trigger and software filters.



9

Fermi Science Menu

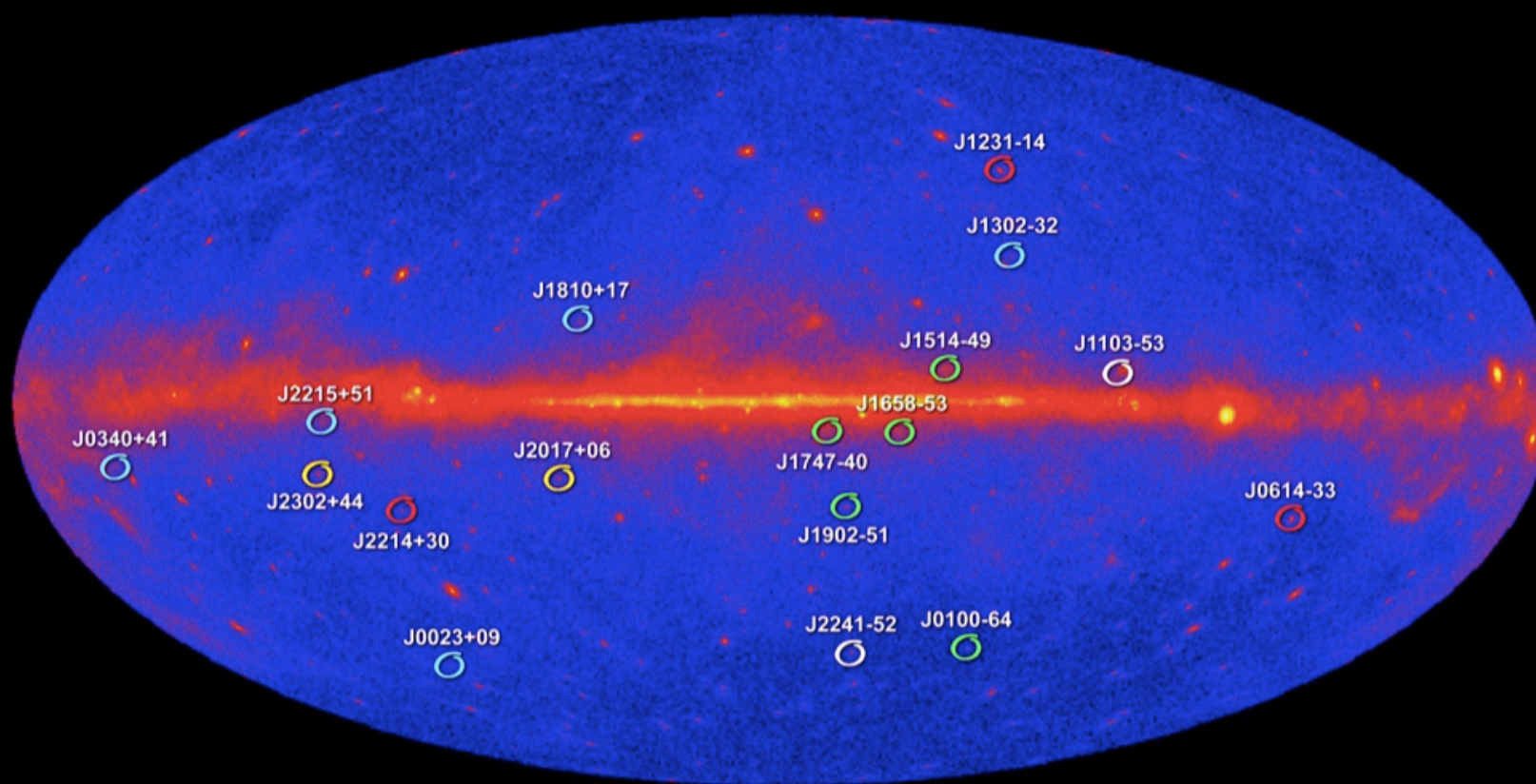


Fermi mission operations: 1) primary mode (sky survey): scan entire sky every 3 hours. 2) Autonomous Repoint Request (ARR) for GRB/transient on-board sw triggers. 3) Target of Opportunity (ToO) following GI proposals/notes. 4) Modified survey profile (e.g. Galactic center biased in Dec.2013-Dec.2014).

Fermi: a tool to study cosmic accelerators
in energy, time, sky position/distribution, cosmic distance

Fermi increased the number of known gamma-ray emitting objects by nearly one order of magnitude compared to previous experiments, and has added several new source classes not previously known in this energy range.

New Millisecond Radio Pulsars Found in Fermi LAT Unidentified Sources



- Led by Fernando Camilo (Columbia Univ.) using Australia's CSIRO Parkes Observatory
- Led by Mallory Roberts (Eureka Scientific/GMU/NRL) using the NRAO's Green Bank Telescope
- Led by Scott Ransom (NRAO) using the Green Bank Telescope
- Led by Ismael Cognard (CNRS) using France's Nançay Radio Telescope
- Led by Mike Keith (ATNF) using Parkes Observatory



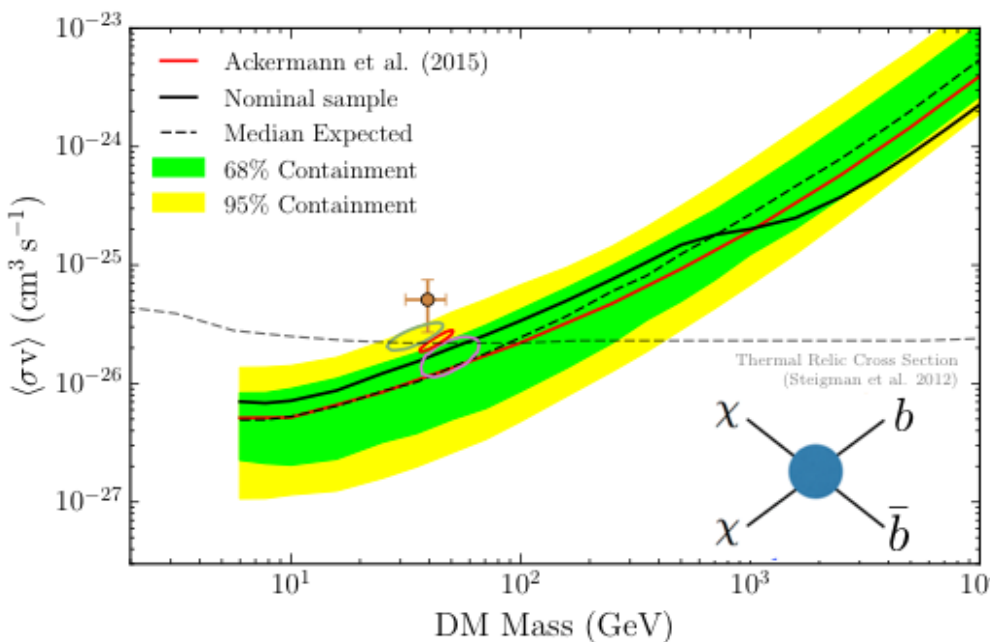
Fermi-LAT limits

$$\frac{d\Phi}{dE_\gamma}(E_\gamma, \psi) = \frac{\langle\sigma v\rangle}{2m_\chi^2} \sum_i B_i \frac{dN_\gamma^i}{dE_\gamma} \frac{1}{4\pi} \int_\psi \frac{d\Omega}{\Delta\psi} \int_{\text{los}} \rho^2(\psi, l) dl$$

Velocity averaged annihilation cross section

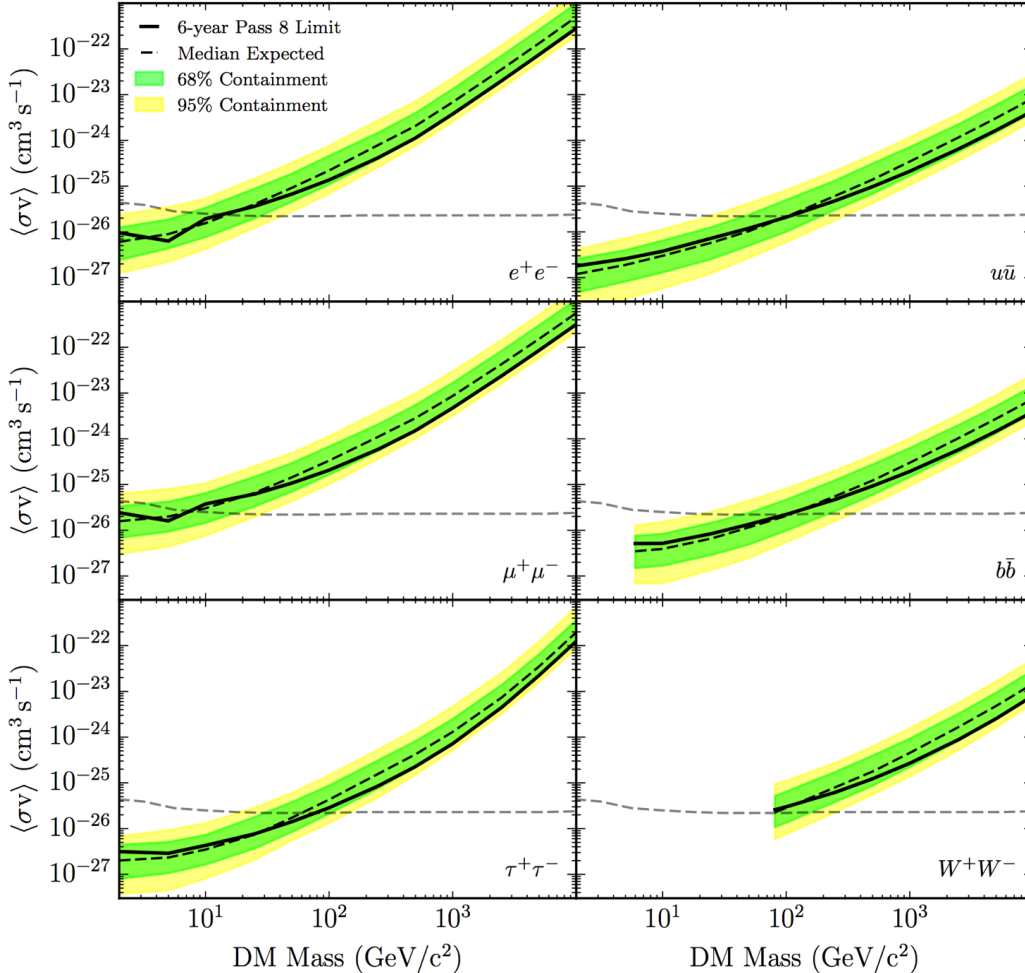
Energy spectra (summing over all the 'i' simplified channels)

J-factor from astrophysical observation



- Limits on the annihilation cross section from gamma rays fluxes
- Fermi-LAT results available only for the $\chi\chi \rightarrow b\bar{b}$ and $\chi\chi \rightarrow \tau\tau$ channels
- *Simplified Models for DM annihilation*
- Experimental data & recipes to calculate upper limits for arbitrary channels provided by Fermi-LAT

Fermi-LAT Results



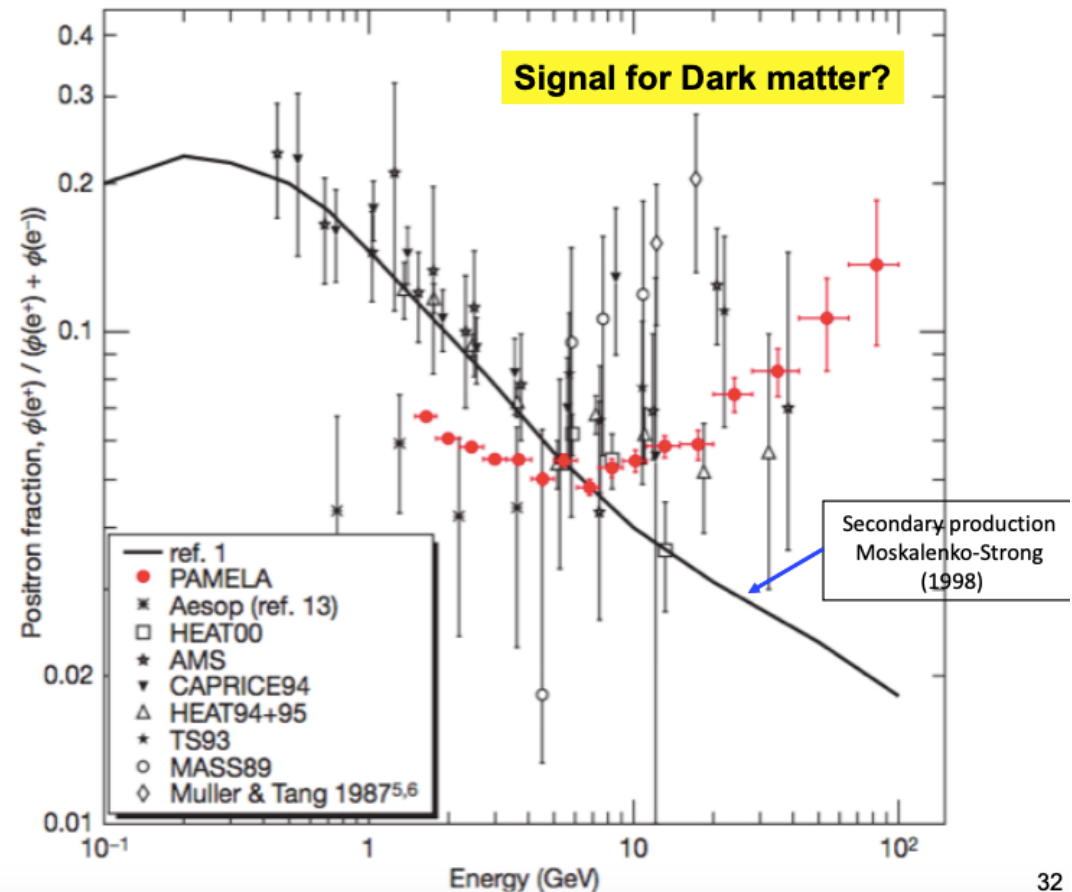
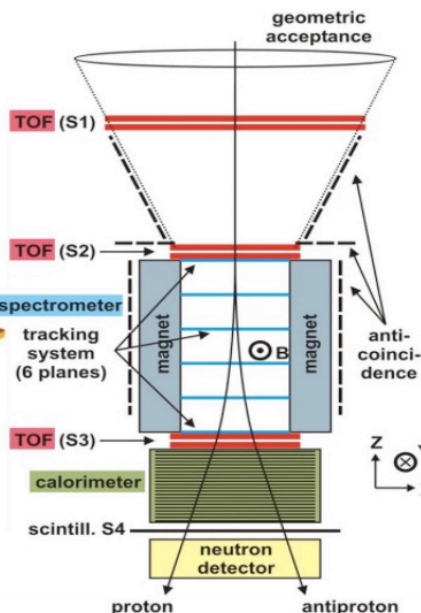
$$\begin{aligned}\chi\chi \rightarrow & gg, q\bar{q}, c\bar{c}, b\bar{b}, t\bar{t}, e^+ e^-, \mu^+ \mu^-, \tau^+ \tau^- \\ & \nu_e \bar{\nu}_e, \nu_\mu \bar{\nu}_\mu, \nu_\tau \bar{\nu}_\tau, ZZ, W^+ W^-, hh\end{aligned}$$

Fermi-LAT upper limits on the velocity-averaged cross section for DM annihilations into several SM channels (simplified models)

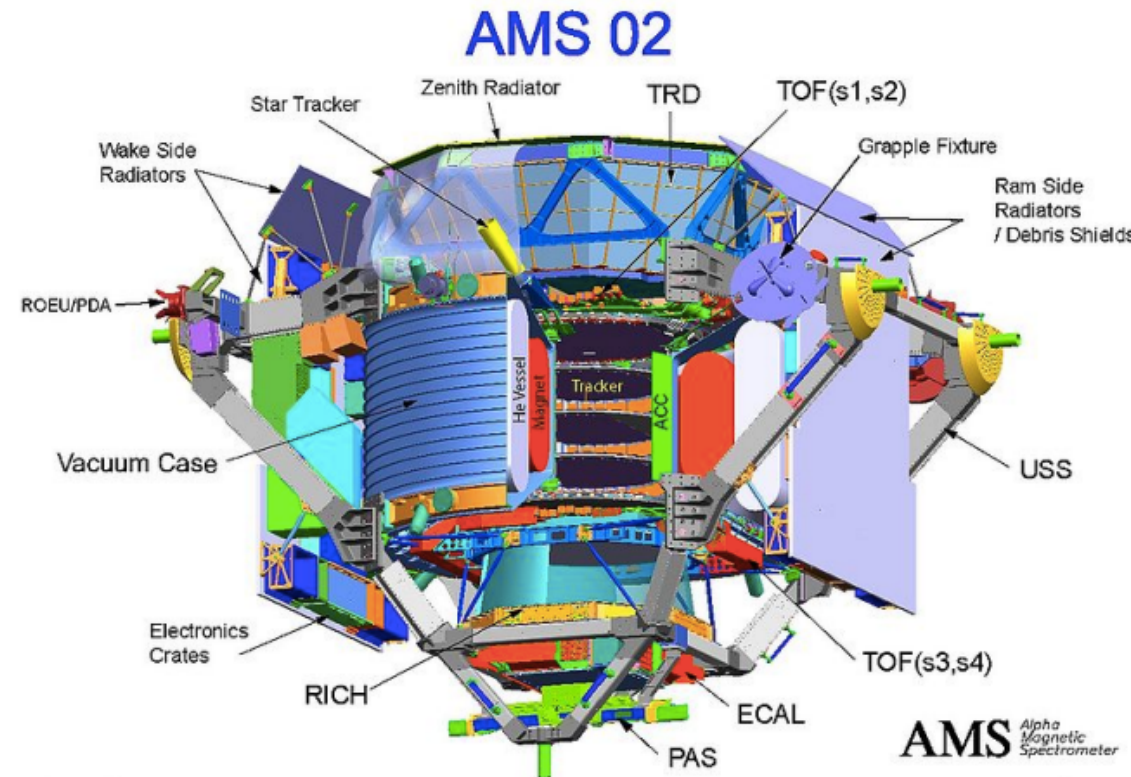
derived using gamma-rays observations from dwarf spheroidal galaxies

PAMELA Instrument

- Satellite-borne instrument.
 - size: 1.02 m (ϕ) x 1.3 m (H)
 - weight: 470 kg
 - power: 355 W
- Time of flight
 - Mass identification up to 1 GeV
- Magnetic spectrometer
 - 0.43 T permanent magnet
 - Silicon strip detector
 - Charge sign and momentum
- Electromagnetic Calorimeter
 - W/Si sampling: $16.3X_0$, $0.6\lambda_L$
 - Electron/positron ID.
 - Energy measurement.



AMS: The Alpha Magnetic Spectrometer

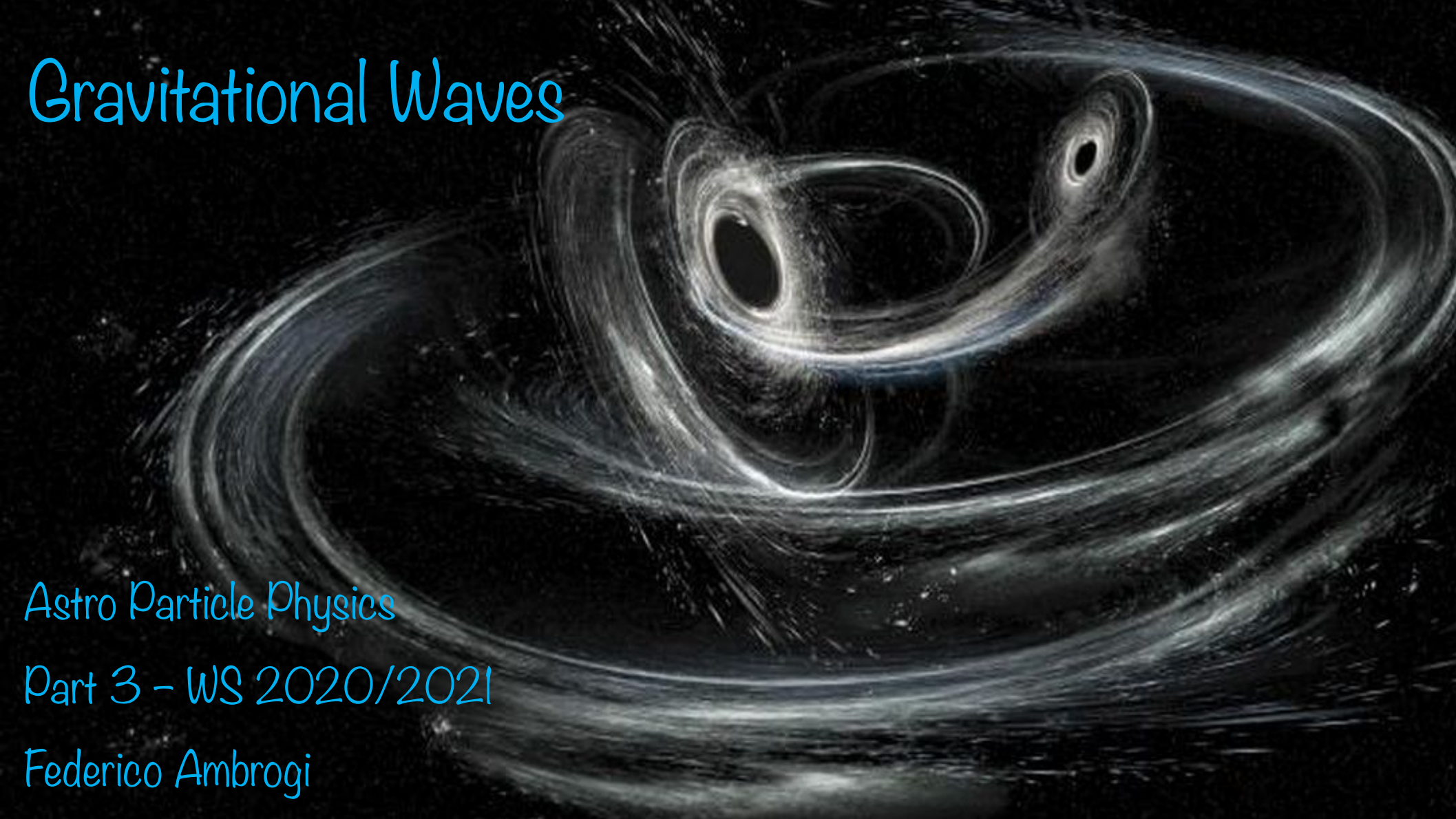


Gravitational Waves

Astro Particle Physics

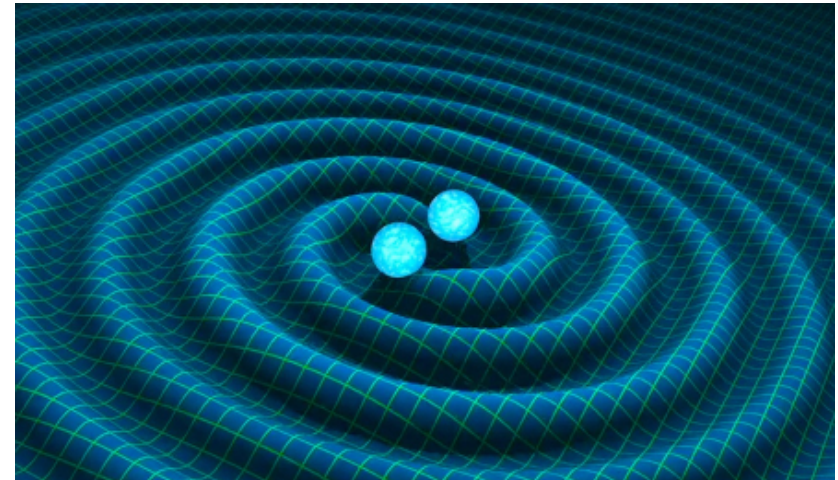
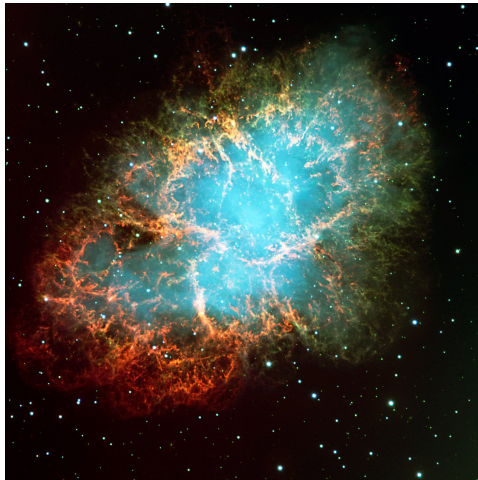
Part 3 - WS 2020/2021

Federico Ambrogi



Gravitational Waves (GWs) represent one of the hot topic in Astrophysics

- Another fundamental proof that Einstein's general relativity is correct
- Give complementary and independent measurements of astrophysical/cosmological parameters
- Allow to observe astrophysical objects/events that cannot be seen with electromagnetic waves or cosmic rays
- Can be used to derive upper limits on some particle properties (e.g. mass of the graviton, strange matter in neutron stars)
- Allow to test the Λ CDM Cosmological Model and the evolution of the universe (e.g. quantum fluctuations, primordial black holes)
- (...)

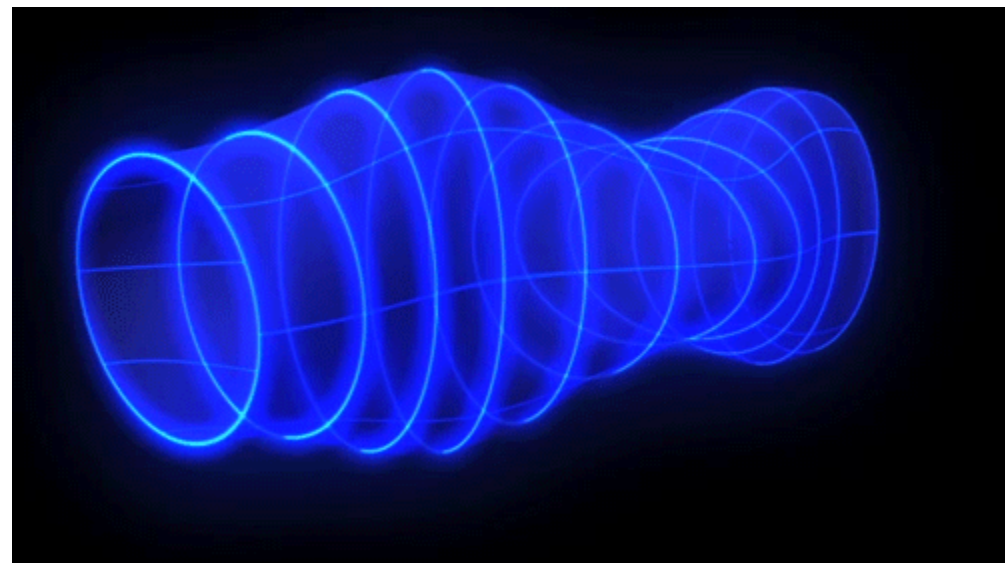
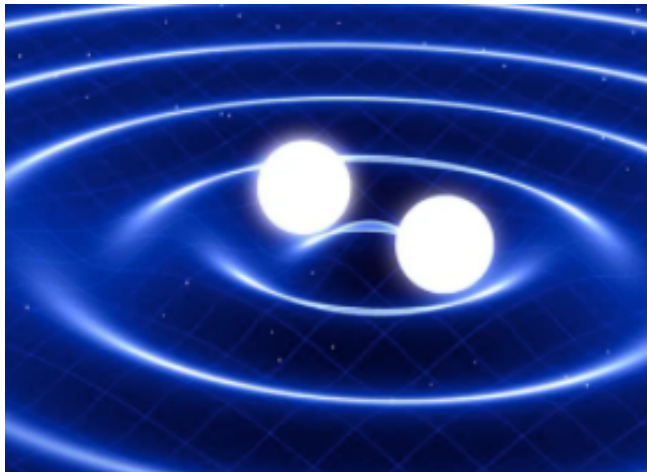


Gws: “ripples” or distortion in the space-time fabric travelling at the speed of light (c) .

- Through their propagation, they distort the space and time around massive bodies or massless particles
- GW change the distance between two fixed points
- The amplitudes and the frequencies of the waves depend on the sources

How do we detect Gws?

What produces Gws?



Theoretical treatment: <https://arxiv.org/abs/1703.00187>

What are Gravitational Waves ?

General Relativity:

$$R_{\mu\nu} - \frac{1}{2} g_{\mu\nu} R = \frac{8\pi G}{c^4} T_{\mu\nu}$$

Search for a solution as a small perturbation h around a Flat Cartesian metric:

$$g_{\mu\nu} = \eta_{\mu\nu} + h_{\mu\nu} \quad \text{with } |h_{\mu\nu}| \ll 1$$

Obtain an equation of waves

$$\square h = -\frac{16\pi G}{c^4} T_{\mu\nu} = 0 \quad \longrightarrow \quad h^{ij}(t, \vec{x}) \sim \frac{2G}{r c^4} \frac{d^2}{dt^2} I^{ij}(t - r/c)$$

Mass monopole:

$$\int \rho(\vec{x}) d^3 \vec{x}$$

Mass energy - conserved

Mass dipole:

$$\int \rho(\vec{x}) \vec{x} d^3 \vec{x}$$

centre of mass energy - conserved

time derivatives vanish

Mass quadrupole:

$$I^{ij} = \int \rho(\vec{x}) \vec{x}^i \vec{x}^j d^3 \vec{x}$$

Moment of inertia - not conserved

What are Gravitational Waves ?

- for a gravitational wave to form, there must be an asymmetry in mass distribution
- GWs are POLARIZED (h_+ , h_x)

Primordial gravitational waves / Quantum fluctuations

Mergers of super-massive black holes (SMBHs, $>10^5$ Msun)

Mergers of compact object binaries

Only GWs observed so far

Mergers of SMBHs and BHs

Neutron stars with crustal asymmetries

Asymmetric supernova explosions

http://web.pd.astro.it/mapelli/lecture1_mapelli.pdf

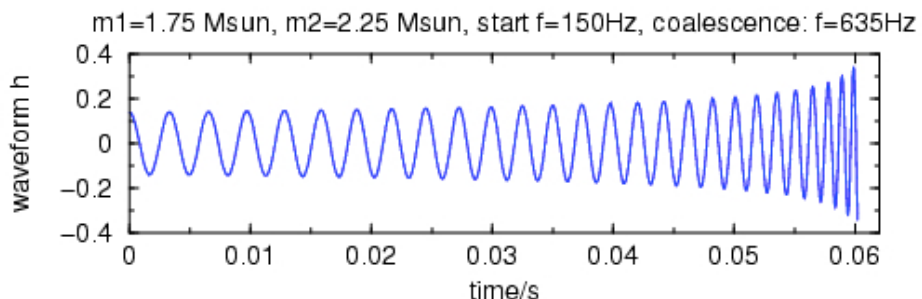
What are Gravitational Waves ?

For binary objects (e.g. two neutron stars)

- the bigger the amplitude (strain), the easier the detection
- the farther the binary, the smaller the amplitude
- the larger the masses, the larger the amplitude
- the smaller the semi-major axis, the larger the amplitude
- emission of GWs implies loss of orbital energy i.e. the binary shrinks while emitting GWs till it merges
- If the binary shrinks ($a \rightarrow 0$), frequency becomes higher
- If the binary shrinks amplitude increases



Gravitational Wave of Compact Binary Inspiral



What are Gravitational Waves ?

“One of the first predictions of General Relativity (GR, 1916)”

<https://www.mdpi.com/2218-1997/2/3/22/pdf>

- Einstein immediately started working on the solution of his field equation in the form of waves
- It took > 50 years to derive generally accepted solutions & the proper equations for the wave forms
- ~1970s: claim by Weber of the observation of GWs (not confirmed by other similar experiments)
- 1974: discovery of the binary system SR B1913+16 (and the Hulse-Taylor binary) → first *indirect* test of Gws emission

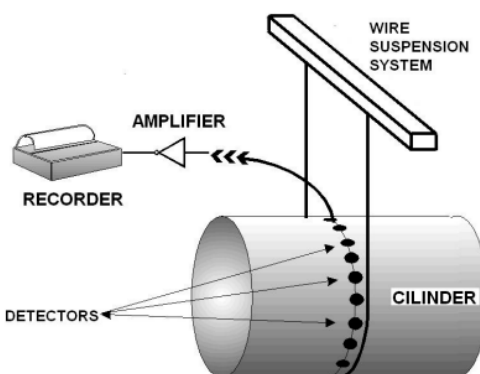


Figure 4. Sketch of Weber's cylinder detector and photo of Joseph Weber at the antenna.



Arecibo (Puerto Rico) telescope: 305-meter radio telescope, world's largest single-aperture telescope (until 2016, with the Chinese FAST telescope)

The Hulse-Taylor Binary Pulsar PSR B1913+16 : indirect discovery of GWs

- Double neutron stars binary system first observed in 1974
- According to general relativity a binary star system should radiate energy in the form of gravitational waves
- Rate of change in orbital period Pb (Peters and Matthews, 1963):

$$\begin{aligned}\dot{P}_b^{\text{GR}} &= -\frac{192 \pi G^{5/3}}{5 c^5} \left(\frac{P_b}{2\pi}\right)^{-5/3} \left(1 + \frac{73}{24}e^2 + \frac{37}{96}e^4\right) (1-e^2)^{-7/2} m_1 m_2 (m_1 + m_2)^{-1/3} \\ &= -1.699451(8) \times 10^{-12} \left[\frac{m_1 m_2 (m_1 + m_2)^{-1/3}}{M_{\odot}^{5/3}} \right]\end{aligned}$$

e=eccentricity

Ratio observation vs prediction accounting for galactic corrections Delta b,gal

$$\frac{\dot{P}_b - \Delta \dot{P}_{b,\text{gal}}}{\dot{P}_b^{\text{GR}}} = 0.997 \pm 0.002.$$

“As we have shown before, this result provides conclusive evidence for the existence of gravitational radiation as predicted by Einstein’s theory.”

<https://arxiv.org/pdf/1011.0718.pdf>

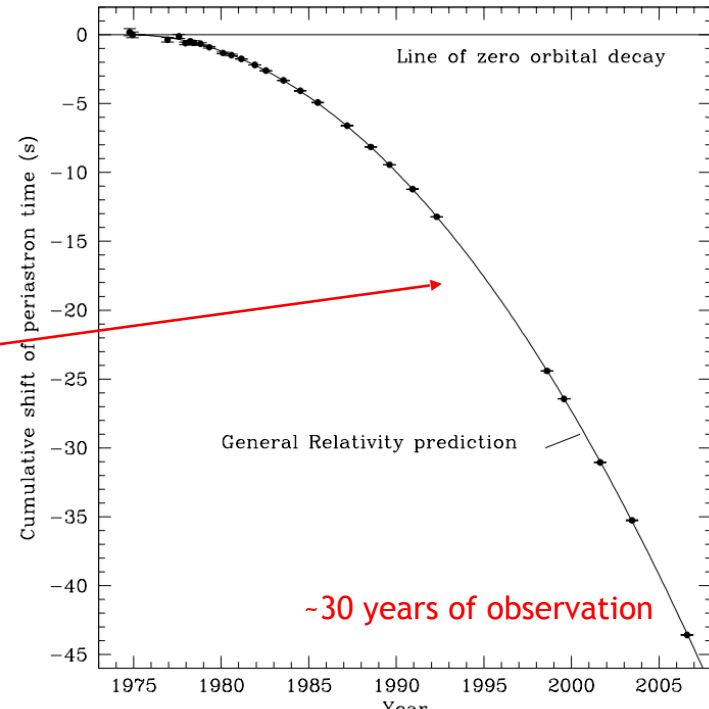


Fig. 2.— Orbital decay caused by the loss of energy by gravitational radiation. The parabola depicts the expected shift of periastron time relative to an unchanging orbit, according to general relativity. Data points represent our measurements, with error bars mostly too small to see.

The Hulse-Taylor Binary Pulsar PSR B1913+16 : indirect discovery of Gas

“One of the first predictions of General Relativity (GR, 1916)”

- Einstein immediately started working on the solution of his field equation in the form of waves
- It took > 50 years to derive generally accepted solutions & the proper equations for the wave forms
- 1974: discovery of the binary system SR B1913+16 (and the Hulse-Taylor binary) → first *indirect* test of GWs emission



1993 Nobel prize to Hulse and Taylor

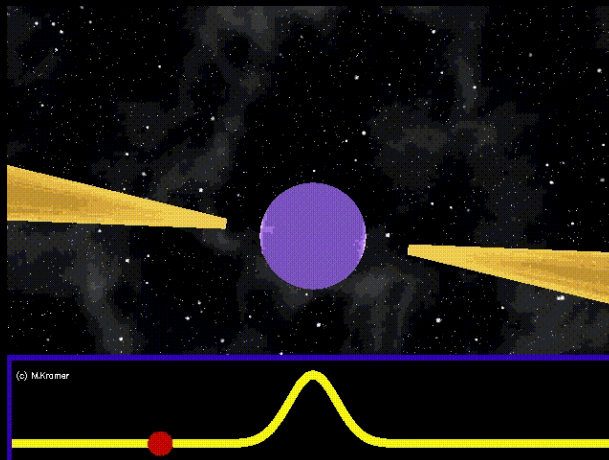
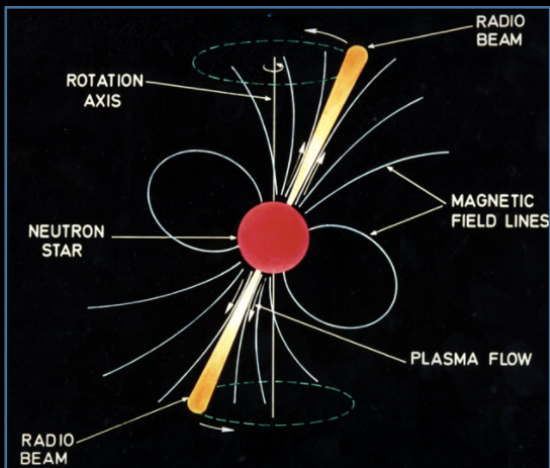
The **Nobel Prize** in Physics **2017**: R. Weiss, B. C. Barish and K. S. Thorne "for decisive contributions to the LIGO detector and the observation of **gravitational waves**."

- 14th September 2015: First observation of GW150914 (event of two black holes merger)
- 17th August 2017: first neutron stars (NSNS) mergers by the Gravitational-Wave Observatory LIGO (LIGO + VIRGO)
- December 2018: catalog of 11 GW events (10 BH , 1 NS) from the first two observation Runs
- O3, Run 3 of observation (LIGO+VIRGO+KAGRA in December 2019)
- O4, Run 4 of observation: delayed to 2022

Pulsars

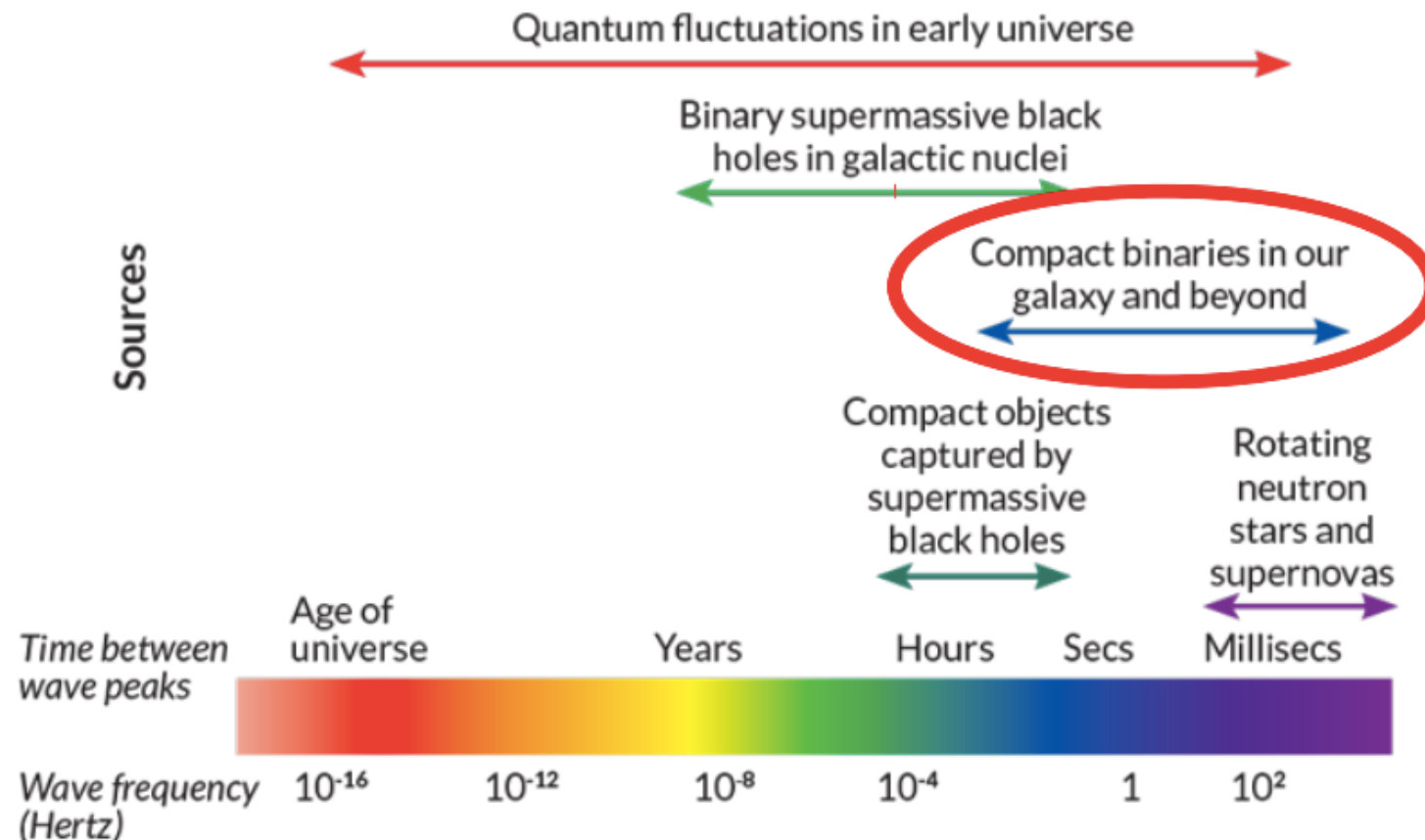
<http://www.jb.man.ac.uk/distance/frontiers/pulsars/section1.html>

- Pulsars (**Pulsating Radio Source**) are rapidly spinning neutron stars
- Their rotation period span from the order of milliseconds to the order of ~8 seconds
- Pulse: collection of radio waves of different frequencies
- Rotation period extremely stable, although the rotation speed slows down with time
- „Lighthouse“ effect



Optical image of the Crab nebula and composite optical/X-ray image of the Crab Nebula, showing synchrotron emission in the surrounding wind nebula, powered by injection of magnetic fields and particles from the central pulsar.

<https://www.ligo.org/science/Publication-S6VSR24KnownPulsar/>



The Interferometers

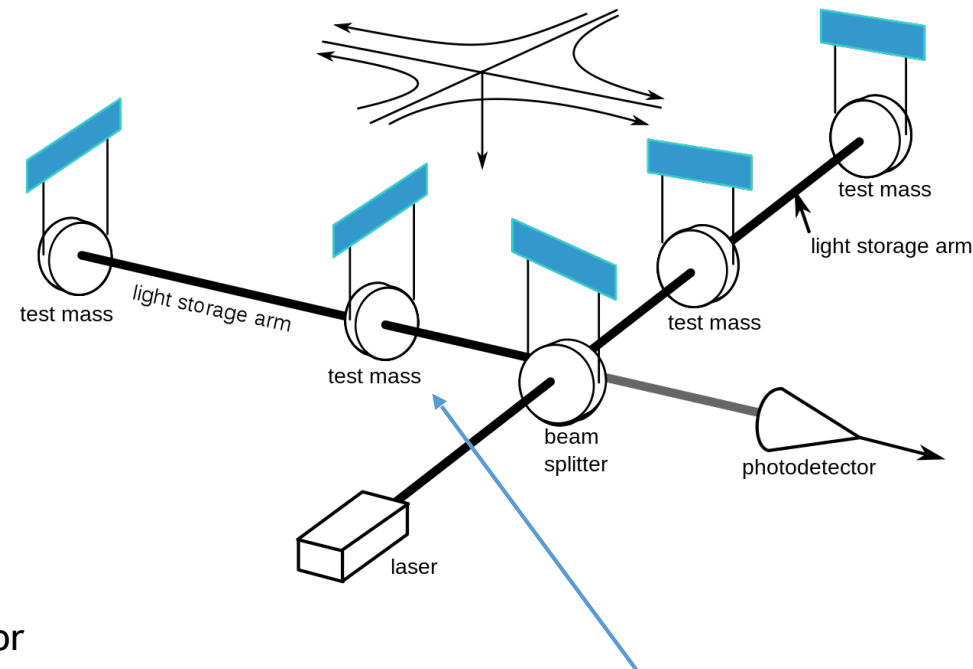
LIGO: the Laser Interferometer Gravitational-Wave Observatory (LIGO)

Handford (Washington) and Livingstone (Louisiana)

VIRGO: Pisa (Italy)

KAGRA: Kamioka Gravitational Wave Detector (Japan)

<https://www.ligo.caltech.edu/page/what-is-interferometer>

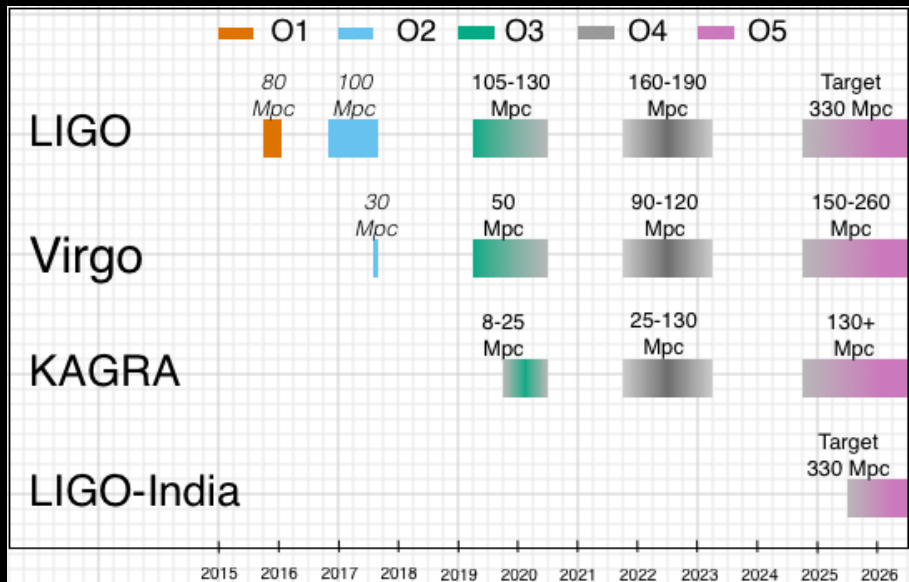
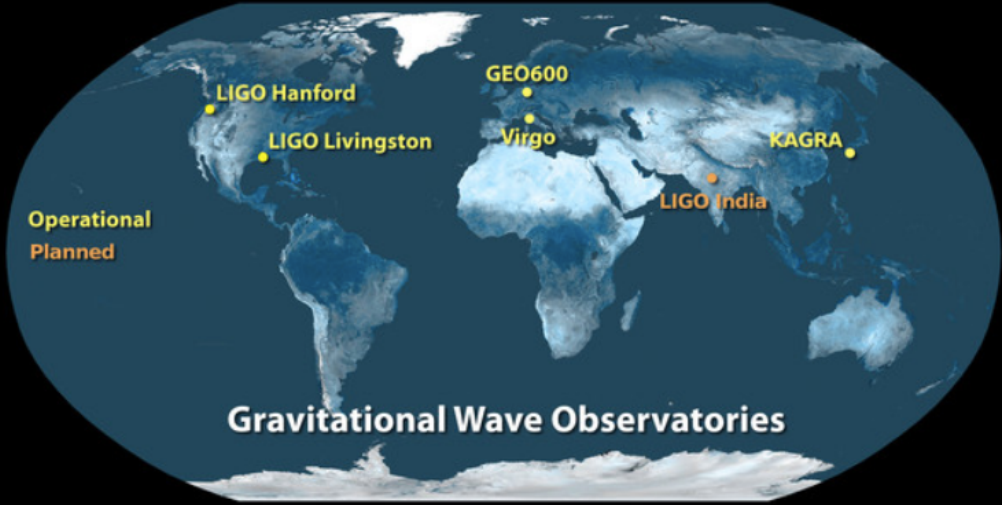


Test masses = mirrors
Their relative position is affected by the passage of the GW

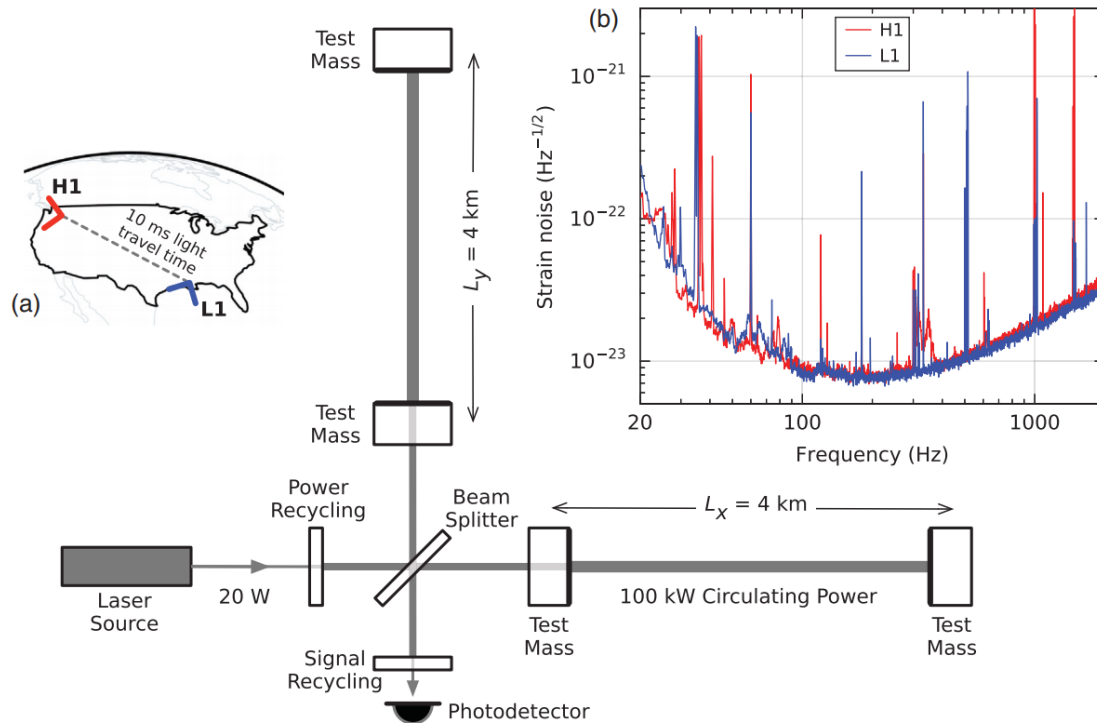
Principles of Michelson's Interferometers

- The passage of gravitational waves, with strain amplitude h (related to the actual amplitude of the GW) causes the modification of the length of the orthogonal arms L_x and L_y ($=4\text{ Km}$) of the interferometer
- An interference pattern will then appear in the photodetector
- The optical signal is proportional to the GW strain
- Nd:YAH laser, 1064 nm; 20kW at source, amplified to 100kW circulating in the arms
- 2nd best vacuum created on Earth (1st: LHC), Pressure < 1 micro Pascal

The Interferometers



The first event: GW150914 (BHBH, Binary Black Holes)

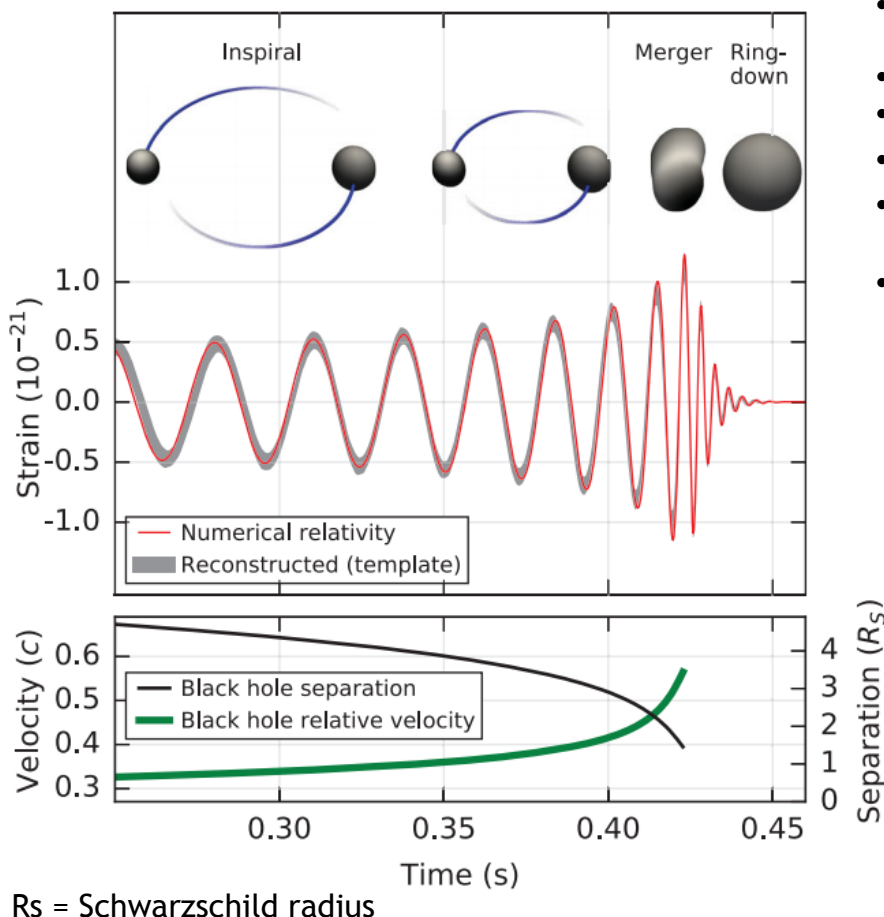


H1: Hanford
L1: Livingston

- Instrumental noise converted to strain amplitude of the instrument close to the time of detection
- strain=relative deformation dL/L
- Peaks correspond to calibration lines, vibration modes of suspension fibers, power grid harmonics
- No environmental disturbances measured by surrounding instruments (seismometers, accelerometers, microphones, magnetometers, radio receivers, weather sensors, ac-power lines monitors, cosmic-rays detectors), fluctuations estimated below 6% of total GW strain
- GWs are searched in the data of the two detectors were the events are compatible with the GW propagation time $H1 \leftrightarrow L1$
- (Note that GW themselves might constitute a background for the measurements)

http://web.pd.astro.it/mapelli/lecture1_mapelli.pdf

The first event: GW150914 (BBH, Binary Black Holes)



- Possible explanation: coalescence of black holes, i.e. their orbital inspiral and merger and final BH ringdown
- Source distance: 410 Mpc (redshift $z = 0.09$)
- Initial black hole masses $36 M_\odot$ and $29 M_\odot$, and the
- Final BH mass is $62 M_\odot$
- Energy of $3 M_\odot c^2$ radiated in gravitational waves
- Also possible to estimate the mass (upper limit) of the associated graviton:

$$m_g < 1.2 \times 10^{-22} \text{ eV}/c^2$$

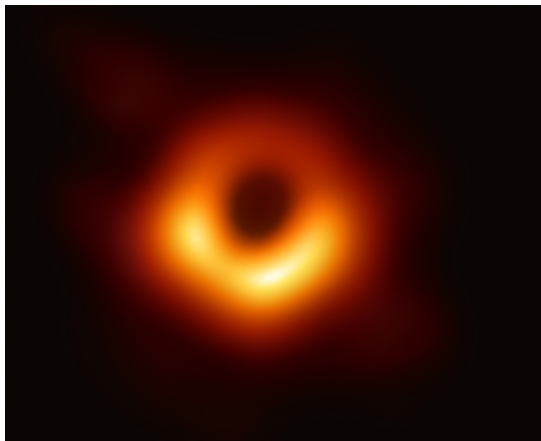
TABLE I. Source parameters for GW150914. We report median values with 90% credible intervals that include statistical errors, and systematic errors from averaging the results of different waveform models. Masses are given in the source frame; to convert to the detector frame multiply by $(1+z)$ [90]. The source redshift assumes standard cosmology [91].

Primary black hole mass	$36^{+5}_{-4} M_\odot$
Secondary black hole mass	$29^{+4}_{-4} M_\odot$
Final black hole mass	$62^{+4}_{-4} M_\odot$
Final black hole spin	$0.67^{+0.05}_{-0.07}$
Luminosity distance	410^{+160}_{-180} Mpc
Source redshift z	$0.09^{+0.03}_{-0.04}$

Since April 10th 2019 : we „see“ them! *Event Horizon Telescope Collaboration*

<https://eventhorizontelescope.org/blog/first-ever-image-black-hole-published-event-horizon-telescope-collaboration>

<https://eventhorizontelescope.org/press-release-april-10-2019-astronomers-capture-first-image-black-hole>



Scientists have obtained the first image of a black hole, using Event Horizon Telescope observations of the center of the galaxy M87. The image shows a bright ring formed as light bends in the intense gravity around a black hole that is 6.5 billion times more massive than the Sun. This long-sought image provides the strongest evidence to date for the existence of supermassive black holes and opens a new window onto the study of black holes, their event horizons, and gravity.

Note: $6.5 \times 10^9 M_{\odot}$ >> than the typical mass of BH detected by gravitational waves $M_{\text{BH}} \approx 40 M_{\odot}$
i.e. two different types of BHs

THE ASTROPHYSICAL JOURNAL LETTERS, 848:L12 (59pp), 2017 October 20

<https://doi.org/10.3847/2041-8213/aa91c9>

© 2017. The American Astronomical Society. All rights reserved.

OPEN ACCESS



Multi-messenger Observations of a Binary Neutron Star Merger

LIGO Scientific Collaboration and Virgo Collaboration, Fermi GBM, INTEGRAL, IceCube Collaboration, AstroSat Cadmium Zinc Telluride Imager Team, IPN Collaboration, The Insight-Hxmt Collaboration, ANTARES Collaboration, The Swift Collaboration, AGILE Team, The 1M2H Team, The Dark Energy Camera GW-EM Collaboration and the DES Collaboration, The DLT40 Collaboration, GRAWITA: GRAvitational Wave Inaf TeAm, The Fermi Large Area Telescope Collaboration, ATCA: Australia Telescope Compact Array, ASKAP: Australian SKA Pathfinder, Las Cumbres Observatory Group, OzGrav, DWF (Deeper, Wider, Faster Program), AST3, and CAASTRO Collaborations, The VINROUGE Collaboration, MASTER Collaboration, J-GEM, GROWTH, JAGWAR, Caltech-NRAO, TTU-NRAO, and NuSTAR Collaborations, Pan-STARRS, The MAXI Team, TZAC Consortium, KU Collaboration, Nordic Optical Telescope, ePESSTO, GROND, Texas Tech University, SALT Group, TOROS: Transient Robotic Observatory of the South Collaboration, The BOOTES Collaboration, MWA: Murchison Widefield Array, The CALET Collaboration, IKI-GW Follow-up Collaboration, H.E.S.S. Collaboration, LOFAR Collaboration, LWA: Long Wavelength Array, HAWC Collaboration, The Pierre Auger Collaboration, ALMA Collaboration, Euro VLBI Team, Pi of the Sky Collaboration, The Chandra Team at McGill University, DFN: Desert Fireball Network, ATLAS, High Time Resolution Universe Survey, RIMAS and RATIR, and SKA South Africa/MeerKAT

Received 2017 October 3; revised 2017 October 6; accepted 2017 October 6; published 2017 October 16

Abstract

On 2017 August 17 a binary neutron star coalescence candidate (later designated GW170817) with merger time 12:41:04 UTC was observed through gravitational waves by the Advanced LIGO and Advanced Virgo detectors. The *Fermi* Gamma-ray Burst Monitor independently detected a gamma-ray burst (GRB 170817A) with a time delay of ~ 1.7 s with respect to the merger time. From the gravitational-wave signal, the source was initially localized to a sky region of 31 deg^2 at a luminosity distance of 40^{+8}_{-8} Mpc and with component masses consistent with neutron stars. The component masses were later measured to be in the range 0.86 to $2.26 M_{\odot}$. An extensive observing campaign was launched across the electromagnetic spectrum leading to the discovery of a bright optical transient (SSS17a, now with the IAU identification of AT 2017gfo) in NGC 4993 (at ~ 40 Mpc) less than 11 hours after the merger by the One-Meter, Two Hemisphere (1M2H) team using the 1 m Swope Telescope. The optical transient was independently detected by multiple teams within an hour. Subsequent observations targeted the object and its environment. Early ultraviolet observations revealed a blue transient that faded within 48 hours. Optical and infrared observations showed a redward evolution over ~ 10 days. Following early non-detections, X-ray and radio emission were discovered at

GW170817 Binary Neutron Stars Merger and Multi-Messenger Astronomy with GWs

H.E.S.S.
High Energy Stereoscopic System



Integral



ALMA



Fermi



Pierre Auger



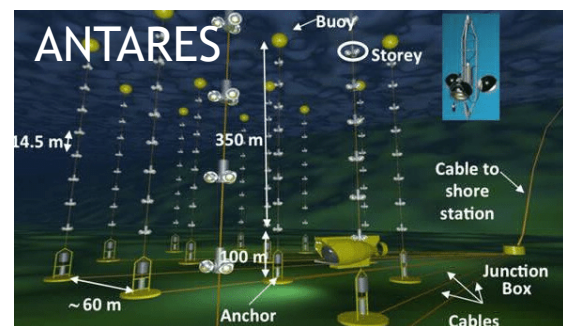
Chandra



LIGO/VIRGO



DES

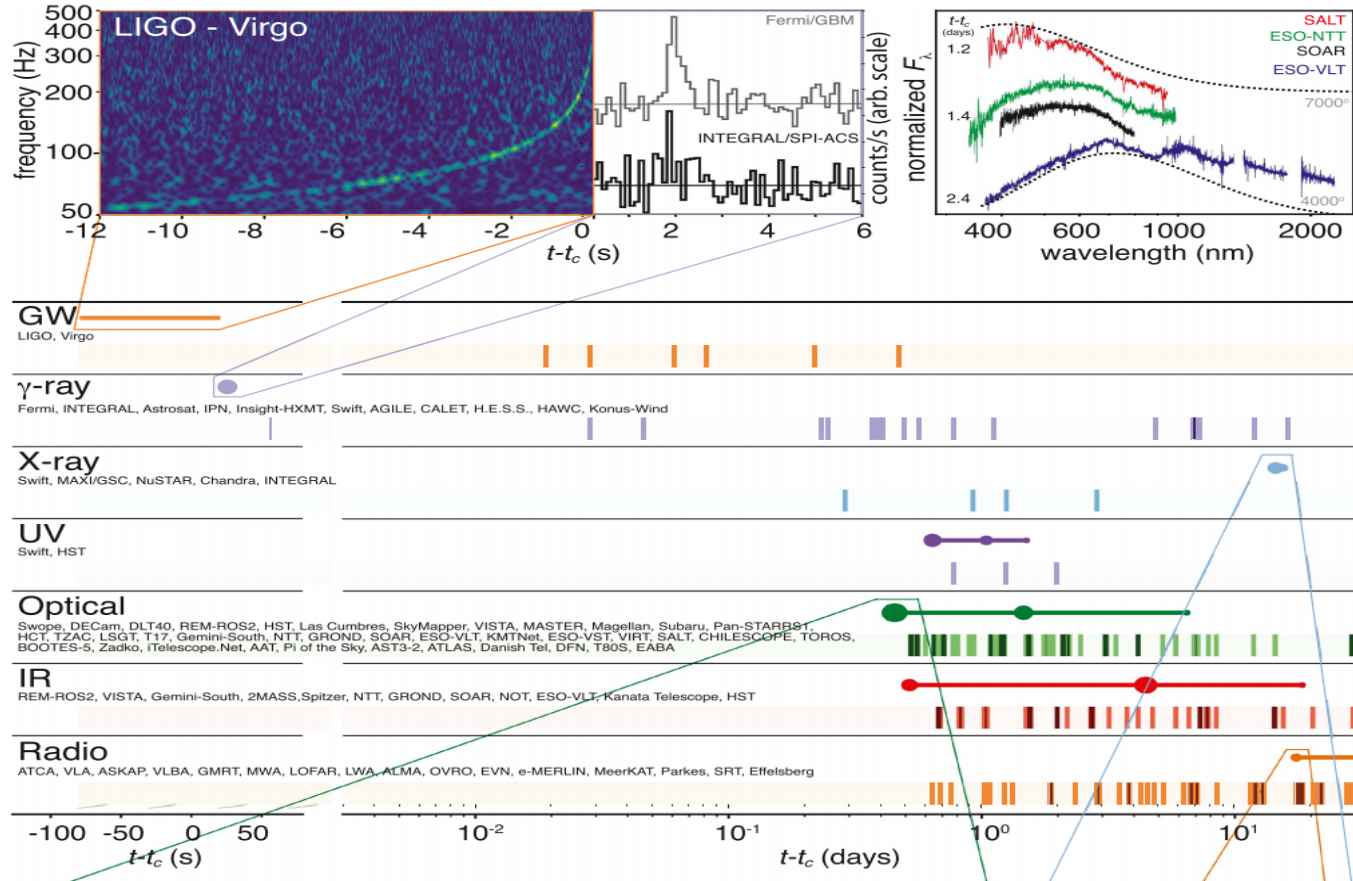


ANTARES



IceCube

GW170817 Binary Neutron Stars Merger and Multi-Messenger Astronomy with GWs



- *First joint detection of gravitational and electromagnetic radiation from a single source*
- ~ 100 s long gravitational-wave signal (GW170817)
- followed by a short Gamma Ray Burst (sGRB, GRB 170817A)
- and an optical transient (SSS17a/AT 2017gfo) found in the host galaxy NGC 4993
- Data compatible with Binary Neutron Stars merger (BNSs), followed by sGRB and a kilonova

$$m_1 \in (1.36-2.26) M_{\odot}$$

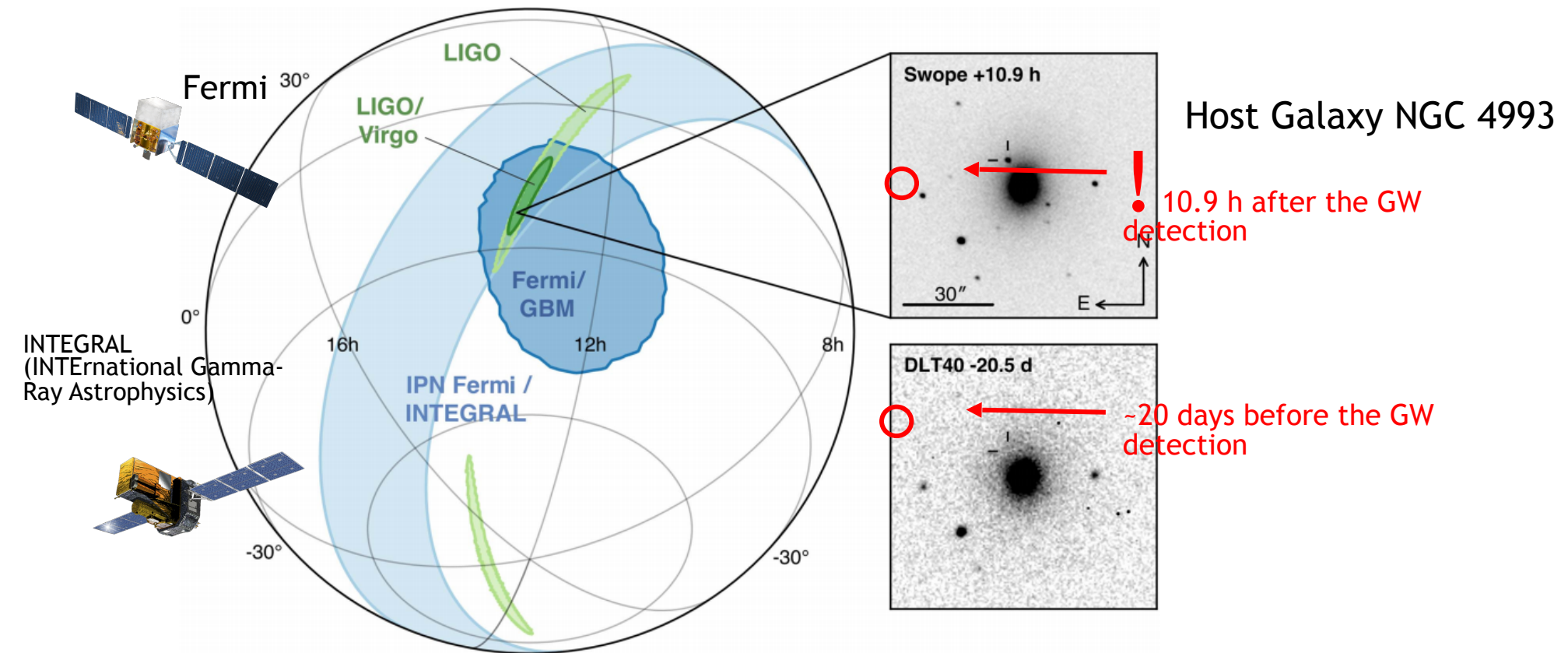
$$m_2 \in (0.86-1.36) M_{\odot}$$

→ $M_{\text{BH}} = 2.82^{+0.47}_{-0.09} M_{\odot}$

Chronology



- On **2017 August 17 12:41:06 UTC** the Fermi GBM onboard flight software triggered on, classified, and localized a GRB. A Gamma-ray Coordinates Network Notice (Fermi-GBM 2017) was issued at **12:41:20 UTC** announcing the detection of the GRB 170817A
- ~ **6 minutes** later, a GW candidate (GW170817) was registered based on a single-detector analysis of the LIGO Hanford data, consistent with a BNS coalescence, with merger time, t_c , **12:41:04 UTC**, less than 2 s before GRB 170817A.
- A GCN Notice was issued at **13:08:16 UTC**. Single-detector gravitational-wave triggers had never been disseminated before in low latency. Given the temporal coincidence with the Fermi-GBM GRB, however, a GCN Circular was issued at **13:21:42 UTC** (LIGO Scientific Collaboration & Virgo Collaboration et al. 2017a) reporting that a highly significant candidate event consistent with a BNS coalescence was associated with the time of the GRB959.
- An extensive observing campaign was launched across the electromagnetic spectrum in response to the Fermi-GBM and LIGO-Virgo detections, and especially the subsequent well-constrained, three-dimensional LIGO-Virgo localization
- A bright optical transient (SSS17a, now with the IAU identification of AT 2017gfo) was discovered in NGC 4993 (at ~40 Mpc) by the 1M2H team SWOPE (**August 18 01:05 UTC**; Coulter et al. 2017a) less than 11 hr after the merger



Besides carrying diverse information, multiple detectors/exp improve the localization of the position of the possible source

The O1/O2 2018 Events Catalog

On December 1, 2018 the LIGO/Virgo Collaboration published a catalog of their searches for gravitational-waves from stellar-mass coalescing compact binaries:

- 10 BBH events
- 1 NSNS event

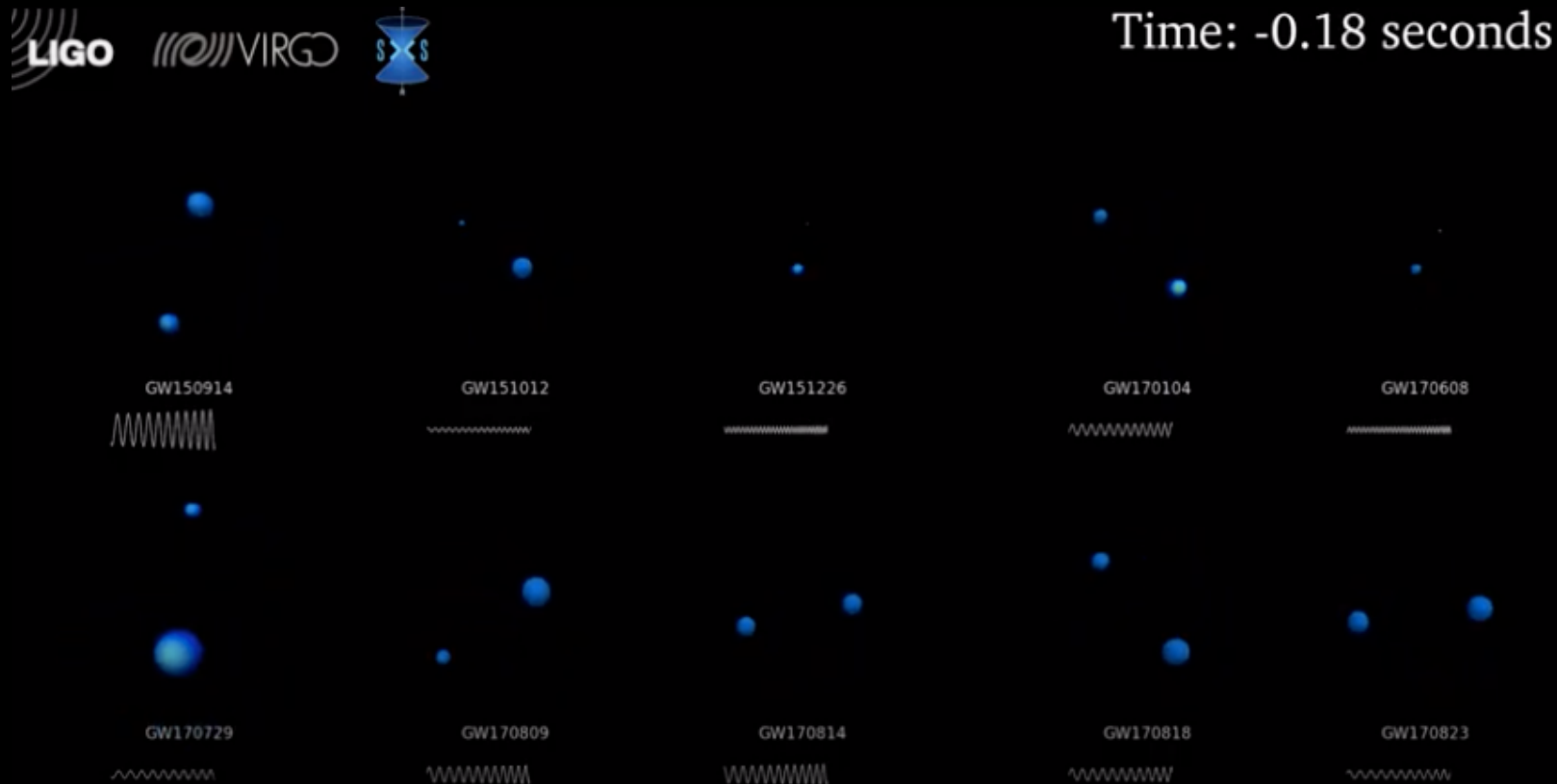
Event	m_1/M_\odot	m_2/M_\odot	\mathcal{M}/M_\odot	χ_{eff}	M_f/M_\odot	a_f	$E_{\text{rad}}/(M_\odot c^2)$	$\ell_{\text{peak}}/(\text{erg s}^{-1})$	d_L/Mpc	z	$\Delta\Omega/\text{deg}^2$
GW150914	$35.6^{+4.8}_{-3.0}$	$30.6^{+3.0}_{-4.4}$	$28.6^{+1.6}_{-1.5}$	$-0.01^{+0.12}_{-0.13}$	$63.1^{+3.3}_{-3.0}$	$0.69^{+0.05}_{-0.04}$	$3.1^{+0.4}_{-0.4}$	$3.6^{+0.4}_{-0.4} \times 10^{56}$	430^{+150}_{-170}	$0.09^{+0.03}_{-0.03}$	179
GW151012	$23.3^{+14.0}_{-5.5}$	$13.6^{+4.1}_{-4.8}$	$15.2^{+2.0}_{-1.1}$	$0.04^{+0.28}_{-0.19}$	$35.7^{+9.9}_{-3.8}$	$0.67^{+0.13}_{-0.11}$	$1.5^{+0.5}_{-0.5}$	$3.2^{+0.8}_{-1.7} \times 10^{56}$	1060^{+540}_{-480}	$0.21^{+0.09}_{-0.09}$	1555
GW151226	$13.7^{+8.8}_{-3.2}$	$7.7^{+2.2}_{-2.6}$	$8.9^{+0.3}_{-0.3}$	$0.18^{+0.20}_{-0.12}$	$20.5^{+6.4}_{-1.5}$	$0.74^{+0.07}_{-0.05}$	$1.0^{+0.1}_{-0.2}$	$3.4^{+0.7}_{-1.7} \times 10^{56}$	440^{+180}_{-190}	$0.09^{+0.04}_{-0.04}$	1033
GW170104	$31.0^{+7.2}_{-5.6}$	$20.1^{+4.9}_{-4.5}$	$21.5^{+2.1}_{-1.7}$	$-0.04^{+0.17}_{-0.20}$	$49.1^{+5.2}_{-3.9}$	$0.66^{+0.08}_{-0.10}$	$2.2^{+0.5}_{-0.5}$	$3.3^{+0.6}_{-0.9} \times 10^{56}$	960^{+430}_{-410}	$0.19^{+0.07}_{-0.08}$	924
GW170608	$10.9^{+5.3}_{-1.7}$	$7.6^{+1.3}_{-2.1}$	$7.9^{+0.2}_{-0.2}$	$0.03^{+0.19}_{-0.07}$	$17.8^{+3.2}_{-0.7}$	$0.69^{+0.04}_{-0.04}$	$0.9^{+0.0}_{-0.1}$	$3.5^{+0.4}_{-1.3} \times 10^{56}$	320^{+120}_{-110}	$0.07^{+0.02}_{-0.02}$	396
GW170729	$50.6^{+16.6}_{-10.2}$	$34.3^{+9.1}_{-10.1}$	$35.7^{+6.5}_{-4.7}$	$0.36^{+0.21}_{-0.25}$	$80.3^{+14.6}_{-10.2}$	$0.81^{+0.07}_{-0.13}$	$4.8^{+1.7}_{-1.7}$	$4.2^{+0.9}_{-1.5} \times 10^{56}$	2750^{+1350}_{-1320}	$0.48^{+0.19}_{-0.20}$	1033
GW170809	$35.2^{+8.3}_{-6.0}$	$23.8^{+5.2}_{-5.1}$	$25.0^{+2.1}_{-1.6}$	$0.07^{+0.16}_{-0.16}$	$56.4^{+5.2}_{-3.7}$	$0.70^{+0.08}_{-0.09}$	$2.7^{+0.6}_{-0.6}$	$3.5^{+0.6}_{-0.9} \times 10^{56}$	990^{+320}_{-380}	$0.20^{+0.05}_{-0.07}$	340
GW170814	$30.7^{+5.7}_{-3.0}$	$25.3^{+2.9}_{-4.1}$	$24.2^{+1.4}_{-1.1}$	$0.07^{+0.12}_{-0.11}$	$53.4^{+3.2}_{-2.4}$	$0.72^{+0.07}_{-0.05}$	$2.7^{+0.4}_{-0.3}$	$3.7^{+0.4}_{-0.5} \times 10^{56}$	580^{+160}_{-210}	$0.12^{+0.03}_{-0.04}$	87
GW170817	$1.46^{+0.12}_{-0.10}$	$1.27^{+0.09}_{-0.09}$	$1.186^{+0.001}_{-0.001}$	$0.00^{+0.02}_{-0.01}$	≤ 2.8	≤ 0.89	≥ 0.04	$\geq 0.1 \times 10^{56}$	40^{+10}_{-10}	$0.01^{+0.00}_{-0.00}$	16
GW170818	$35.5^{+7.5}_{-4.7}$	$26.8^{+4.3}_{-5.2}$	$26.7^{+2.1}_{-1.7}$	$-0.09^{+0.18}_{-0.21}$	$59.8^{+4.8}_{-3.8}$	$0.67^{+0.07}_{-0.08}$	$2.7^{+0.5}_{-0.5}$	$3.4^{+0.5}_{-0.7} \times 10^{56}$	1020^{+430}_{-360}	$0.20^{+0.07}_{-0.07}$	39
GW170823	$39.6^{+10.0}_{-6.6}$	$29.4^{+6.3}_{-7.1}$	$29.3^{+4.2}_{-3.2}$	$0.08^{+0.20}_{-0.22}$	$65.6^{+9.4}_{-6.6}$	$0.71^{+0.08}_{-0.10}$	$3.3^{+0.9}_{-0.8}$	$3.6^{+0.6}_{-0.9} \times 10^{56}$	1850^{+840}_{-840}	$0.34^{+0.13}_{-0.14}$	1651

TABLE III. Selected source parameters of the eleven confident detections. We report median values with 90% credible intervals that include statistical errors, and systematic errors from averaging the results of two waveform models for BBHs. For GW170817 credible intervals and statistical errors are shown for IMRPhenomPv2NRT with low spin prior, while the sky area was computed from TaylorF2 samples. The redshift for NGC 4993 from [87] and its associated uncertainties were used to calculate source frame masses for GW170817. For BBH events the redshift was calculated from the luminosity distance and assumed cosmology as discussed in Appendix B. The columns show source frame component masses m_i and chirp mass \mathcal{M} , dimensionless effective aligned spin χ_{eff} , final source frame mass M_f , final spin a_f , radiated energy E_{rad} , peak luminosity ℓ_{peak} , luminosity distance d_L , redshift z and sky localization $\Delta\Omega$. The sky localization is the area of the 90% credible region. For GW170817 we give conservative bounds on parameters of the final remnant discussed in Sec. V E.

<https://www.ligo.org/science/Publication-O2BBHPop/flyer.pdf>

The 01/02 2018 Events Catalog

<https://www.youtube.com/watch?v=9xY53UyQjQs>



Masses in the Stellar Graveyard

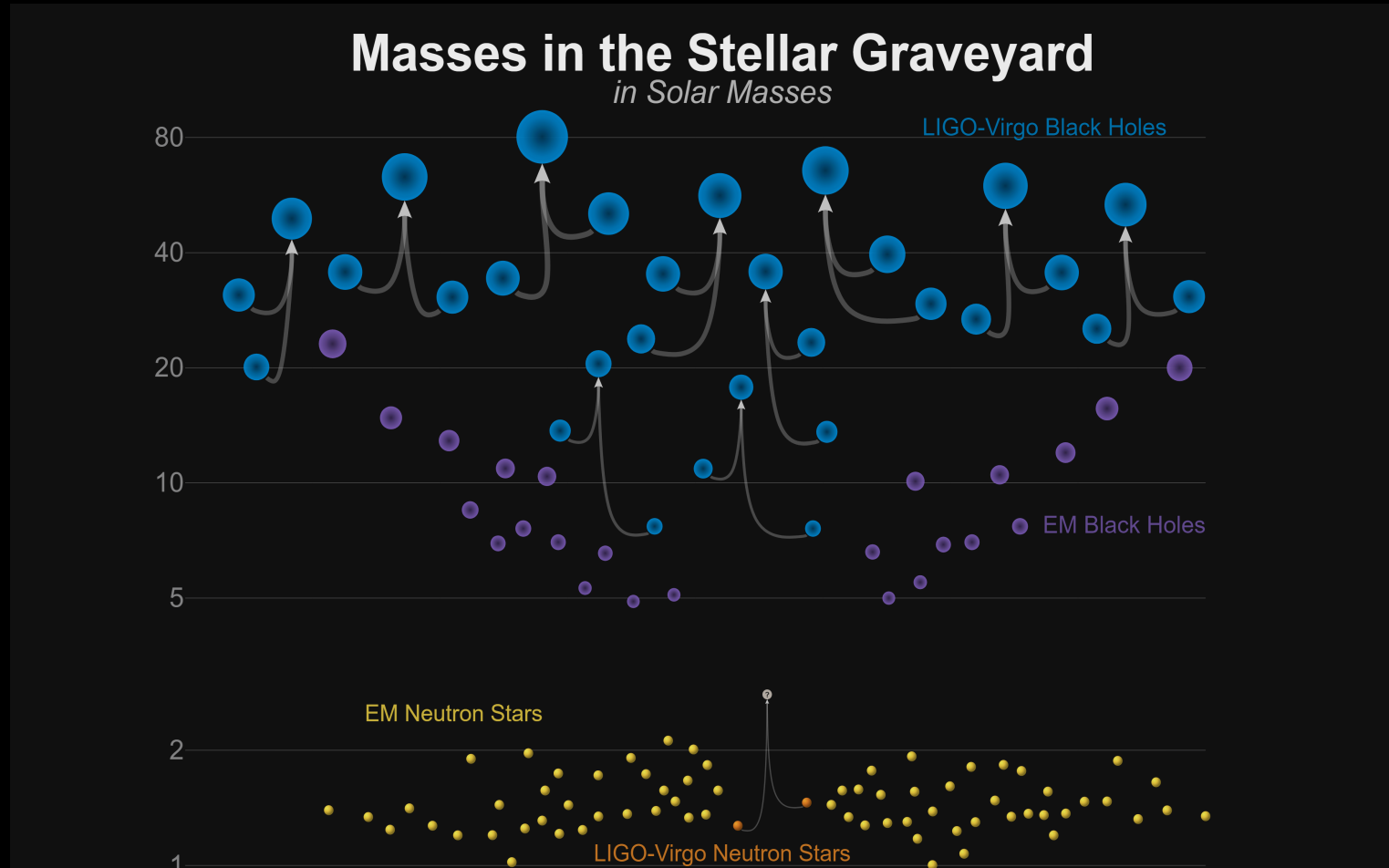
in Solar Masses

LIGO-Virgo Black Holes

EM Black Holes

EM Neutron Stars

LIGO-Virgo Neutron Stars

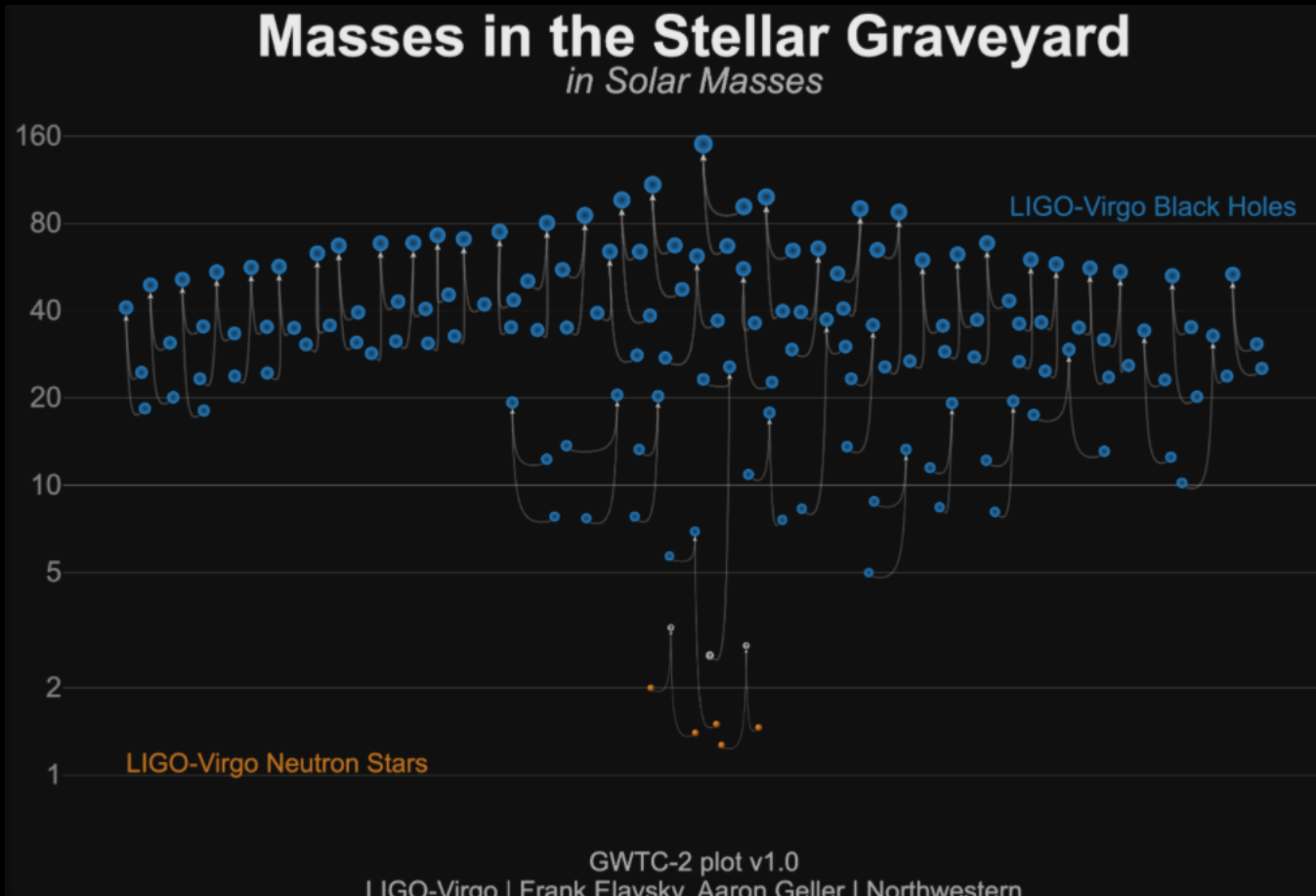


GWTC-2: AN EXPANDED CATALOG OF GRAVITATIONAL-WAVE DETECTIONS

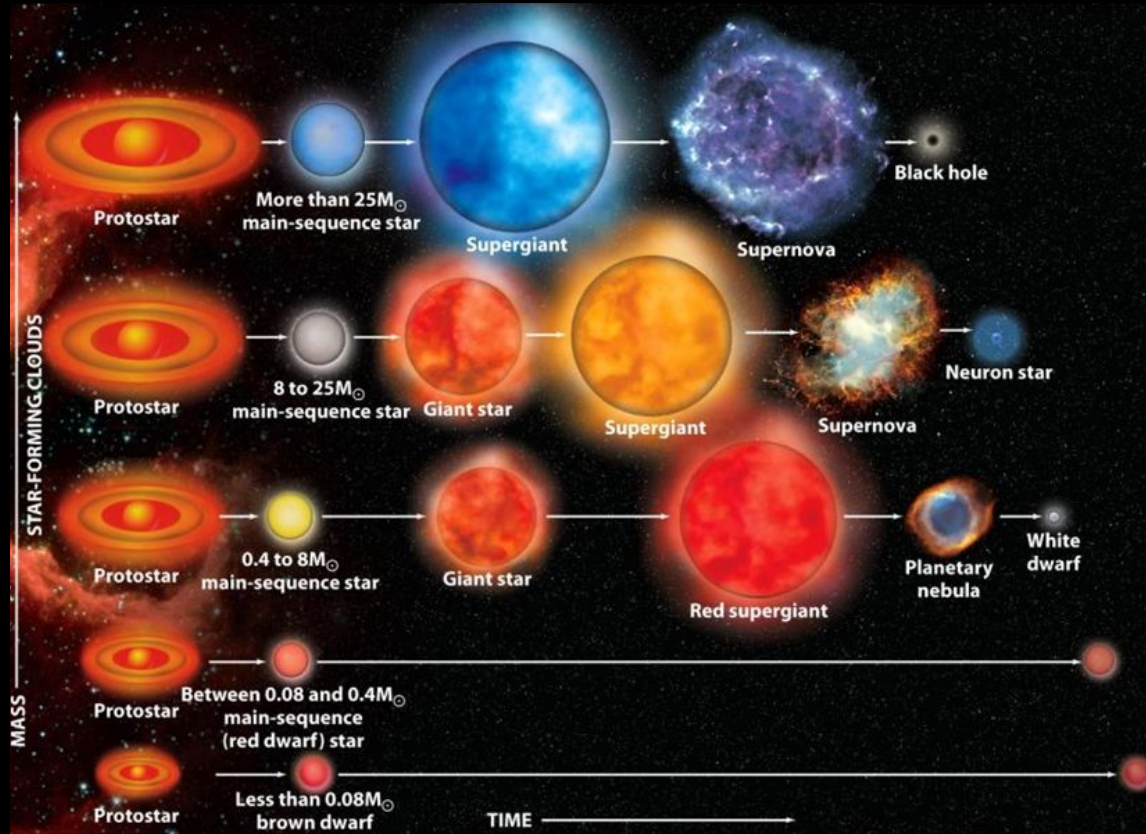
<https://www.ligo.org/science/Publication-O3aCatalog/>

Dated 28 October 2020
50 GWs events
(BHBH, NSBH, NSNS)

Some especially interesting O3a events include the second ever gravitational-wave observation consistent with a binary neutron star merger, the first events with unequivocally unequal masses, and a very massive black hole binary with a total mass of about 150 times the mass of the Sun.



Stellar Evolution (i.e. Where BHs and NSs come from)



Take home

Star evolution mostly depends on the mass of the original gas cloud

Metallicity i.e. chemical composition impacts fusion processes

For initial mass $M_i > 0.08 M_{\odot}$ → white dwarfs

For $M_i > 8 M_{\odot}$ → Supernova (SN) explosion and NS remnant

For $M_i > 8 M_{\odot}$ → SN explosion and formation of BHs (fallback or direct)

Stellar evolution end with the creation of White Dwarfs, SNe, Neutron Satrs, Black Holes which are sources of gravitational waves!

[Typical numbers of neutron star:

Mass $\sim 1.4 M_{\odot}$

radius ~ 10 Km

magnetic field 10^{12} Gauss (LHC: 4 T = 40k Gauss, average in Milky way \sim microGauss, Earth surface \sim 0.2 Gauss)]

GWs as a test for Cosmology/Evolution of the Universe/Stellar Evolution

- It is possible to use the properties of the sources of the GWs observed to constrain Cosmology and evolution models
- It is possible to set upper limits, with a certain confidence level (here 90%) on the number of events per volume of universe per unit of time
- GW170817 used as a *Standard Sirene* (see next)

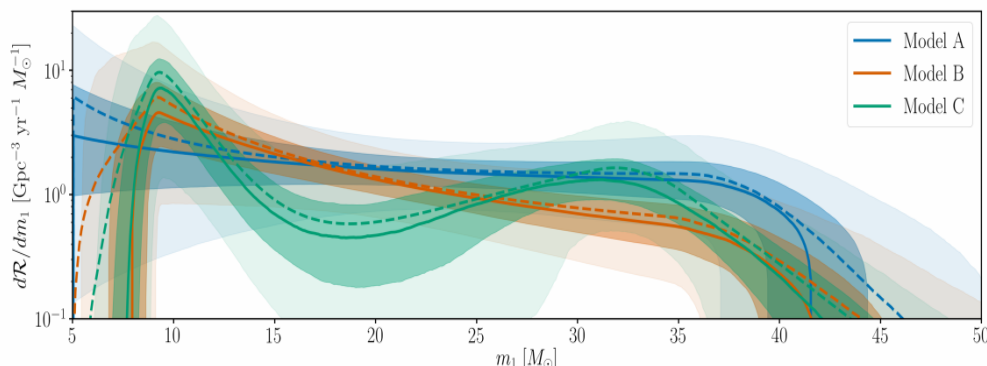


Figure 2: The number of black holes of a given mass which participate in mergers over a given volume of space, for a few different model assumptions. Model A has the least amount of complexity and Model C is the most complex. The solid lines, dark shades, and light shades show the median, 50%, and 90% credible intervals, and the dashed line shows the ‘posterior population distribution’, or best prediction for what mass a typical population member might have. Adapted from Figure 1 in the paper.

“GW measurements of black holes have already had profound implications for stellar astrophysics. Most black holes are heavier than the previously known population of stellar-mass black holes from EM obs. of X-ray binary systems; this told us something about how and where heavy BBHs might have formed. “

<https://www.ligo.org/science/Publication-O2BBHPop/index.php>

The Future: Space Interferometers

Laser Interferometer Space Antenna (LISA) mission of the European Space Agency

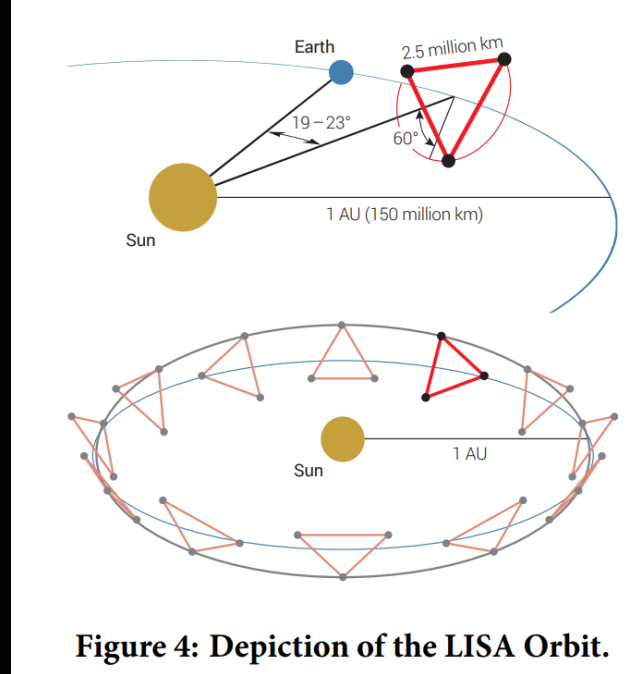
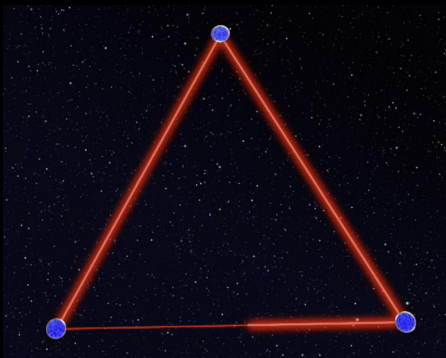


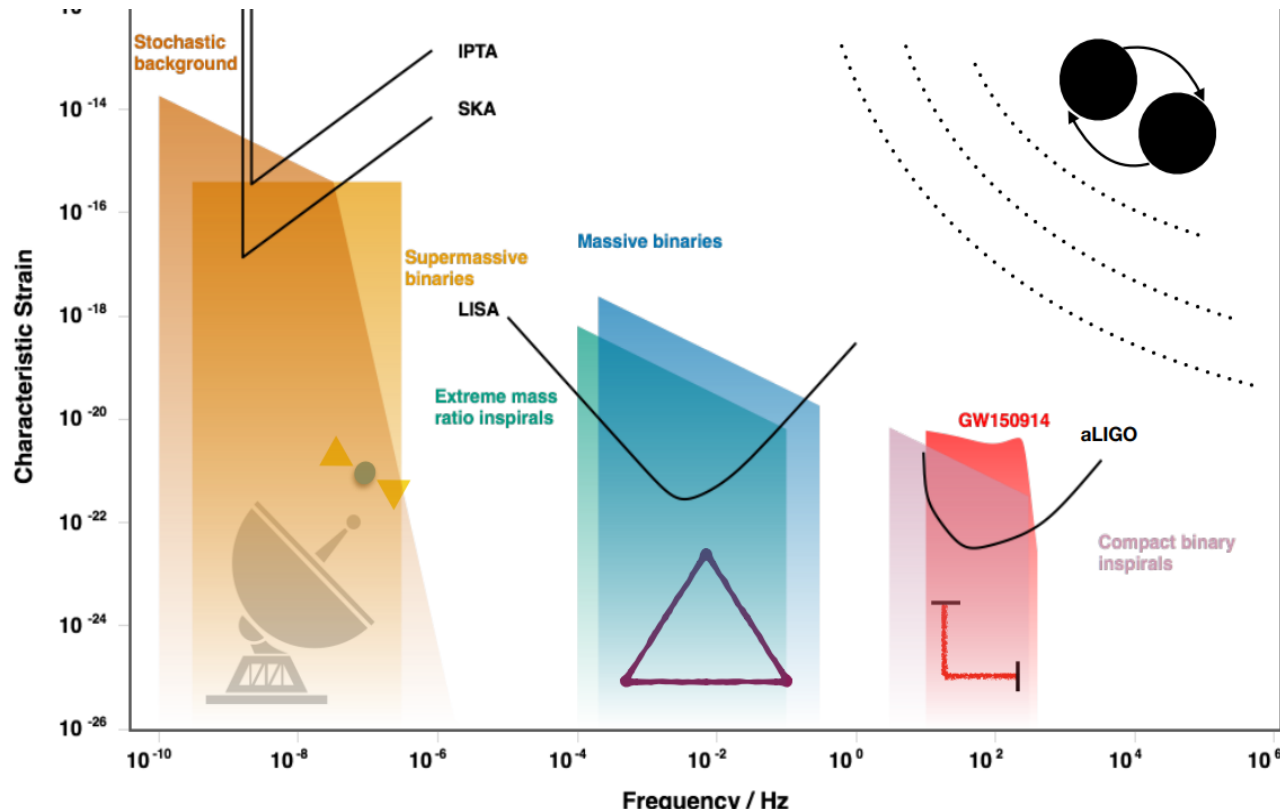
Figure 4: Depiction of the LISA Orbit.

- First dedicated space-based gravitational wave detector
- Three spacecraft arranged in an equilateral triangle with sides 2.5 million km long, flying along an Earth-like heliocentric orbit
- Each of the spacecraft contains two telescopes, two lasers and two test masses (each a 46 mm, 2 kg, gold-coated cube of gold/platinum)
- 2.5 million km corresponds to 8.3 seconds

http://www.esa.int/Science_Exploration/Space_Science/A_unique_experiment_to_explore_black_holes
https://www.elisascience.org/files/publications/LISA_L3_20170120.pdf

The Future: Space Interferometers

<https://arxiv.org/pdf/1806.06979.pdf>



- With LISA it will be possible to observe e.g. BBHs months to week before the actual merger with great accuracy in determining the position in the sky
- The actual merger could be then detected by aLIGO
- This makes it possible to follow the merging events in time
- EMRI (extreme mass ratio inspirals): e.g. BH of $\sim 50 M_\odot$ inspiraling around a massive BH ($\sim 10^6 M_\odot$) that should be common in the galactic centres
- Gravitational waves background (e.g. from Inflation, phase transitions, spontaneous symmetry breaking)